UNIVERSIDAD DE ALCALÁ Y

UNIVERSIDAD REY JUAN CARLOS

MASTER OFICIAL EN HIDROLOGÍA Y GESTIÓN DE RECURSOS HÍDRICOS

PROYECTO DE FIN DE MÁSTER

SENSORES DE AGUA LIMPIA DE BAJO COSTE BASADOS EN CÉLULAS SOLARES FOTOVOLTAICAS (CLEAN WATER PV SENSORS)

AUTORA:
Marta Vivar García

DIRECTORES:
Dra. Irene de Bustamante Gutiérrez (UAH)
Dr. Eloy García Calvo (UAH)

Alcalá de Henares, 24 de Mayo de 2013

Dña. Irene de Bustamante Gutiérrez, profesora titular de Geodinámica Externa, y D. Eloy García Calvo, profesor catedrático de Ingeniería Química, como tutores del **proyecto de fin de máster titulado: "Sensores de agua limpia de bajo coste basados en células solares fotovoltaicas (Clean Water PV sensors)",** damos nuestro **Visto Bueno** a la presentación y la lectura de la memoria del proyecto en la convocatoria de Mayo de 2013.

Fdo.: Irene de Bustamante

Fdo.: Eloy García Calvo

AGRADECIMIENTOS

A mis directores de proyecto, Irene y Eloy, por la confianza y el apoyo para estudiar temas nuevos. Por el optimismo.

A mis compañeros del máster, por ayudarme cuando estaba perdida y cuando no he podido ir a clase. Que siga la curiosidad por las cosas.

A Gabriel Sala del Instituto de Energía Solar de Madrid, por compartir siempre ideas y dejarme utilizar los laboratorios como si fuera mi casa. Por las células, la silicona y las horas de soldadura. A Miguel, por su entusiasmo en el taller y su ayuda.

A Carlos del Cañizo, Ana y Carlos de Centesil, por ayudarme a cortar las células de este proyecto y escuchar con paciencia infinita.

A Matt, por los datos completos de un año en Chipre donde hace sol, y por los días de frío en el norte de Italia.

A Jorge y Gustavo, de la Universidad de Jaén, por los días de medida al sol y por la alegría que llevan.

A Raquel y MªÁngeles, por los días de laboratorio en IMDEA, por compartir la ilusión de hacer experimentos al sol con agua. Por todo lo que me enseñan.

Y a mi familia y amigos, por estar ahí y cuidarme siempre.

Y a Manuel, claro. Por todo.

TABLE OF CONTENTS

INDEX OF FIGURES

INDEX OF TABLES

INDEX OF ACRONYMS

UV: Ultraviolet

WT: Water Treatment

PV: Photovoltaic

SODIS: Solar Disinfection

UVA: Ultraviolet-A

SWP: Solar Water Pasteurization

WHO: World Health Organisation

WAPI: Water Pasteurization Indicator

CIGS: Copper Indium Gallium (di) Selenide

CdTe – Cadmium Telluride

STC: Standard Testing Conditions

AM: Air Mass

MPP: Maximum Power Point

ECT: Equivalent Cell Temperature

WMO: World Metereological Organisation

SD: Sunshine Duration

VIS: Visible

NIR: Near-Infrared

PET: Polyethylene terephthalate

LGBC: Laser-Grooved Buried Contact

Abstract

Currently 708 million people lack access to a safe water supply, most of them in rural areas with limited infrastructures and resources. Unsafe water and poor sanitation cause 80% of all diseases in the developing world. This project is focused on the development of simple, cost-effective, easy to operate and maintain, and socially acceptable domestic water purification units. It is a challenge that requires the application of scientific knowledge from various disciplines.

Solar disinfection technologies use the bactericidal effect of UV radiation or convert the solar energy into heat for pasteurization. But their widespread is highly affected by efficiency, cost and reliability. Natural UV water treatment (WT) only uses 5% of the total available solar energy, limiting the system efficiency dramatically and increasing the cost. And all solar WT lack low-cost sensors to detect when the water is clean, reducing their 'usability' in developing regions.

We will develop low-cost clean water sensors suitable for all solar disinfection technologies by using PV solar cells that can measure received irradiance and water temperature based on their current and voltage. No sensors based on this idea have been built or considered yet despite the plummeting of silicon technologies costs and their potential high impact.

1. INTRODUCTION

About 708 million people lack access to clean drinking water according to the most recent update from the World Health Organisation [1], with almost all of them in developing regions. From this world population without drinking water sources, 84 % live in rural areas. As an example, in India, 1.9 million children die every year; 20 percent of these deaths result from diarrhoea-related diseases, which are usually caused by unsafe drinking water and poor sanitation [1]. On the other hand, emergency situations such as floods and earthquakes also produce lack of water supply, often in areas with limited access to infrastructure and resources [2].

Criteria for the development of a successful water treatment (WT) method in rural areas in developing countries and emergency situations are very similar: simple, low cost, appropriate for domestic use, easy to operate and maintain, low environmental impact, low energy requirements, no strong supply chain requirements, high potential social acceptance and high performance [2,3,4]. Main water treatment processes include: a) boiling, simple and efficient but it requires firewood (high energy usage); b) chlorine disinfection, very effective, simple and inexpensive, but it needs continuous chemical supply and it forms toxic gases (harmful and environmentally damaging); c) filtration, simple but not effective with all contaminants and with high maintenance; d) reverse osmosis, very effective but with very high cost and high energy usage; d) artificial UV radiation, very efficient but also expensive and requiring specialised parts (UV lamps); and d) solar disinfection, clean, simple, but environmental dependent and in some cases with very low performance.

Solar disinfection technologies have been proven as one of the most appropriate point-of-use WT methods [5, 6], especially in remote regions with high irradiance conditions (most of the developing countries are located in the so-called ‘sun-belt’) and either restricted or unavailable access to electrical power and/or chemical supplies. They can use directly the bactericidal effect of UV radiation [7] or convert the solar energy into heat for thermal pasteurization or distillation, or a combination of both. Main solar technologies include (Fig. 1): natural UV disinfection using photocatalytic reactors, solar pasteurization systems reaching water temperatures of about 70ºC, solar distillation by water evaporation and condensation, and direct exposure of plastic bottles following the SODIS process [5] for a certain number of hours combining UV radiation and heat.

(a)

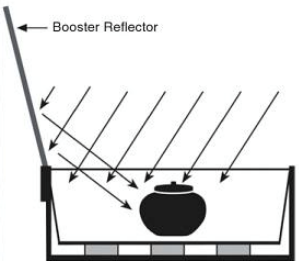

(b)

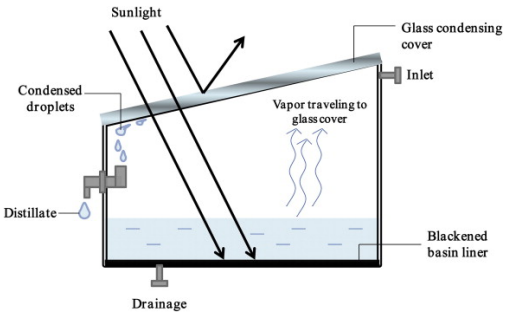

(c)

(d)

Fig. 1: Solar Water Treatment (WT) methods: a) Natural UV disinfection using photocatalytic reactors (PSA-CIEMAT, Almeria, Spain), b) Solar pasteurization [6], c) Solar distillation [2], d) SODIS process [5].

But their widespread is hampered due to efficiency, cost and reliability limitations:

a) Efficiency and cost limitations. Natural UV water treatments only use the UV components of the solar spectrum, which constitutes only 5% of the total available solar energy, limiting the system efficiency dramatically and increasing the cost. This is especially critical for photocatalytic reactors, as most of the simple, cheap and stable photocatalysts are active only in the UV and near UV region. Other limitations include surface area restrictions due to the relatively small available surface of the photocatalyst when it is coated on the photoreactor walls [6, 8]; and energy limitations, as the system needs some source of electricity to feed the pumps and maintain the system, which adds also more complexity. Very substantial research efforts are being conducted across the international scientific community to overcome these technological limitations including: extending the absorption of photocatalysts into the visible part of solar spectra [9, 10]; or increasing the effective photocatalytic surface areas by developing new nanostructures such as nanofibers, nanotubes or graphene particles suspended in water [8, 11]. However, there are also potential drawbacks such as the decrease in corrosion resistance of photocatalysts as spectral absorption is increased, causing an unfortunate trade-off between

performance and longevity; and dispersing nanoparticles in the water introduces an additional separation step for the removal of the nanoparticles from the purified water which is expensive, complex, and not suitable for rural areas in developing countries. Another approach is to increase the total efficiency of the system by using the full solar spectrum more efficiently, developing low-cost hybrid photovoltaic-photocatalytic systems for the generation of electricity and clean water in a single unit [12, 13]. This new technology is currently under development and the potential is yet to be fully explored.

b) Reliability limitations. All solar disinfection technologies lack low-cost sensors to detect when the water is clean, i.e. if the treated water has received enough radiation and/or if it has reached the pasteurization temperature. This lack of information reduces their 'usability' in remote regions. Scientific research is currently looking for all type of low-cost simple sensors that can provide some aid to detect when the water is clean, both for solar UV disinfection and solar water pasteurization:

1. *Solar UV disinfection sensors*: UVA dosimetric indicators (Fig. 2a) using azo dyes such as Mehtylene Blue or Acid Orange AO24 are currently being developed. These sensors are based in the complete discolouration of the dye when it degrades after receiving the solar radiation dose for inactivation of pathogens [14, 15, 16]. When the indicator is in the dark and in the presence of oxygen, it is reoxidised back to methylene blue, constituting a reversible system.

2. *Solar water pasteurization (SWP) sensors*: One type of SWP indicator is based on melting of a wax from solid to liquid and then changing shape or location, such as the WAPI (Water Pasteurization Indicator) shown in Fig. 2b [6, 17]. The WAPI is a polycarbonate tube containing a wax at the top that melts at 69° C. It is placed inside a water container under SWP, and when the water reaches pasteurization temperature the heat will melt the wax, that will move from the top to the bottom of the tube, indicating that pasteurization has been completed.

   Another pasteurization indicator is based on materials with different thermal expansions that could interact and make a change in geometry [6], such as a bi-metal disc that due to different thermal expansions of the two metals will change its shape into a different position.

The only technology that would not need an indicator is solar distillation, but it requires higher solar energy doses for longer periods of time to purify water than any of the other solar technologies [6].

(a) (b)

Fig. 2: a) UVA dosimetric indicator showing the discolouration when the UV dose required for pathogen inactivation has been received [16], b) WAPI indicator, showing the wax location before and after reaching pasteurization temperature [17].

This project will address the problem of the low reliability of solar water technologies for developing regions due to the lack of low-cost clean water sensors. A ***new type of low-cost sensors can be developed using photovoltaic (PV) solar cells that provide information about received irradiance and temperature***. No sensors based on this idea have been built yet despite the plummeting of silicon technologies costs (PV modules are less than 1€/Wp) and their potential high impact in solar water treatment.

The structure of the project is as follows: first, we will introduce the fundamentals of photovoltaic solar cells and their potential application as clean water sensors according to the solar water technologies requirements (Chapter 2), such as measuring global irradiance or estimating sunshine hours (Chapter 3), UV irradiance and water temperature. Then we will focus on the design of the clean water PV sensor (Chapter 4), reviewing the previous developed sensors based on solar cells in other fields prior to the design itself of the PV sensor. Once the design is completed, materials, manufacturing and initial charaterisation will be described. Chapter 5 will be dedicated to the different tests conducted under real sun with SODIS technology to characterise the sensor performance. Main results and achievements will be discussed. We will finalise with conclusions and future work in Chapter 6.

2. PV SOLAR CELLS AS CLEAN WATER SENSORS: PRINCIPLES OF OPERATION AND SOLAR WATER TECHNOLOGIES

This chapter describes the basics of photovoltaic solar cells and their potential application for measuring global irradiance, and/or estimating sunshine hours, UV irradiance and water temperature, which are parameters that are useful to determine the end of a water purification process when using solar energy. Main requirements from the different solar water technologies are also reviewed in order to understand their key parameters and facilitate the designing the sensor.

2.1 Principles of operation of photovoltaic solar cells

A photovoltaic solar cell is an electronic device that converts the incident sunlight into electricity. It is made by a semiconductor material that when receives sunlight produces electron-hole pairs that originate current and voltage (Fig. 3a). Depending on the band gap of the semiconductor material, the efficiency of the cell will vary, as only photons with sufficient energy (above the band gap) will contribute to electricity generation.

The most common semiconductor material used in solar cells is silicon, which can be grown monocrystalline, multicrystalline or amorphous. There are also other type of solar cells including thin films (CIGS – Copper Indium Gallium (di) Selenide, CdTe – Cadmium Telluride) and concentrator solar cells (multijunction solar cells – InGaP - InGaAs - Ge).

Fig. 3b shows a monocrystalline solar cell manufactured by the Spanish company Isofotón. This cell has a rated efficiency of 18.5% at Standard Testing Conditions (STC), which are defined by international standards (IEC 61215 [18]) at 1000W/m^2 of solar irradiance (spectrum AM1.5G) and 25ºC of cell temperature. It is 156mm x 156mm and it provides an output power of 4.4W. Considering this low value, multiple solar cells need to be connected together in photovoltaic modules (Fig. 3c) in to build sufficient power (145W for the PV module of the example) for real world applications.

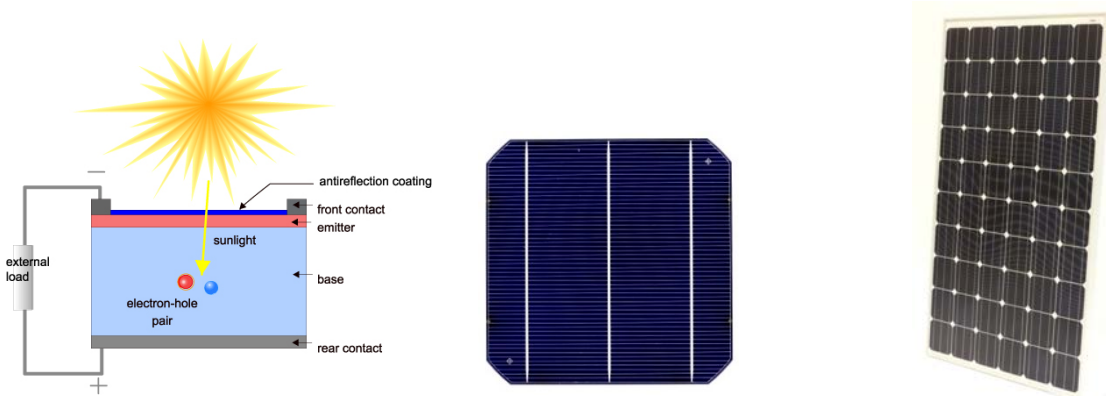

(a) (b) (c)

Fig. 3: a) Principle of operation of a solar cell when receiving sunlight, showing the generation of electron-hole pairs which originate current and voltage [19], b) Solar cell from manufacturer with a rated power of 4.4W [20], c) Photovoltaic module composed by 36 solar cells, with a rated power of 145W [20].

The electrical characteristics of current-voltage (I-V) of a solar cell under operation (illumination) are shown in Fig. 4. The power delivered to an external load is the product of the current by the voltage. The equation of the cell is given by Eq. I:

$$I \cong I_{SC}\left(1 - exp\frac{q(V-V_{OC})}{mkT}\right) \qquad Eq.\ I$$

where I is the current, I_{SC} is the short-circuit current (maximum current from the cell that occurs when the voltage across the cell is zero), V is the voltage, V_{OC} is the open-circuit voltage (maximum voltage from the cell that occurs when the current across the solar cell is zero), m is the linearity factor of the cell (usually equal to 1), q is the charge of the electron (1.602×10-19 C), k is the Boltzmann constant (1.38×10-23 J/K) and T is the operating temperature of the cell in K (at standard test conditions for solar cells the temperature is 25°C or 300K).

From the I-V curve and the general equation of the solar cell, we have the **main operating parameters of the cell**:

- Short-circuit current, I_{SC}, already defined.
- Open-circuit voltage, V_{OC}, also defined.

- Power at the maximum power point (MPP), P_{MPP}, power at the point where the product of the voltage (V_{MPP}) and current (I_{MPP}) is maximum. This is the optimum point of operation of the cell.
- Efficiency of the cell, η, which is the ratio between the power output and the power input. The power output is the maximum power and the power input is the solar irradiance falling on the solar cell.

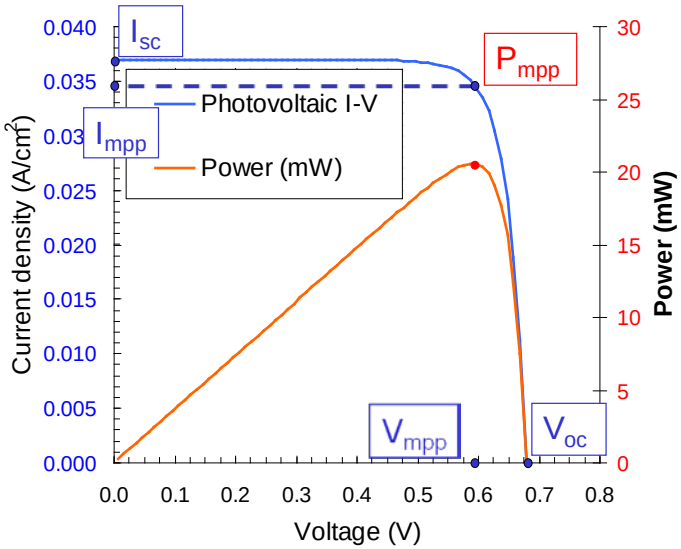

Fig. 4: I-V curve of a solar cell (in blue) and power-voltage characteristic (in red), showing the main parameters of a solar cell: short-circuit current (I_{SC}), open-circuit voltage (V_{OC}), maximum power point (P_{MPP}), maximum power point current (I_{MPP}) and maximum power point voltage (V_{MPP}) [21].

From these parameters, we will focus in this project on the short-circuit current (I_{SC}) and the open-circuit voltage (V_{OC}) and their variations with irradiance and temperature.

2.2 Effect of irradiance and temperature on I_{SC} and V_{OC}

The **light intensity** has an important effect in the operating parameters of a solar cell. The generated photo-current and voltage will be different if the solar irradiance changes.

Specifically, for the short-circuit current, it will increase almost linearly with a higher irradiance, and for the open-circuit voltage, it will increase as a logarithmic function. Eq. II and III show the variation of I_{SC} and V_{OC} with irradiance:

$$I_{SC} \cong \frac{G}{G^*} I_{SC}^* \qquad \textit{Eq. II}$$

where G is the irradiance, G^* is the irradiance at STC conditions (1000W/m^2), and I_{SC}^* is the short-circuit current of the cell at STC.

$$V_{OC} = V_{OC}^* + \frac{mkT}{Q} ln \frac{G}{G^*} \qquad \textit{Eq. III}$$

where G is the irradiance, G^* is the irradiance at STC conditions (1000W/m^2), and V_{OC}^* is the open-circuit voltage of the cell at STC.

Eq. III also shows that the open-circuit voltage changes with the **operating cell temperature**. Under similar irradiance conditions, we can use the open-circuit voltage temperature coefficient β to calculate the variation of V_{OC} with temperature (Eq. IV):

$$V_{OC}(T) = V_{OC}(25℃) + \beta(T - 25℃) \qquad \textit{Eq. IV}$$

where $V_{OC}(25℃)$ is the open-circuit voltage at 25°C (STC), β is the open-circuit voltage temperature coefficient (for silicon solar cells is approximately -2.3mV/°C), and T is the cell operating temperature.

On the other hand, the short-circuit current is considered to have such small variation with temperature that usually we assume that it is constant with temperature (Eq. V):

$$I_{SC} \cong I_{SC}^* \qquad \textit{Eq. V}$$

Therefore, using these variations of I_{SC} and V_{OC}, we can use the solar cells to measure directly irradiance and cell temperature.

2.2.1 I_{SC} measurement as irradiance sensor

From Eq. II, we can see that by measuring I_{SC} and knowing the I_{SC} at standard conditions we can measure the solar irradiance falling on the solar cell, so it serves as an irradiance sensor (Eq. VI):

$$G = G^* \frac{I_{SC}}{I^*_{SC}} \qquad \textit{Eq. VI}$$

Fig. 5 shows the set-up for measuring the I_{SC} of a cell. We use a calibrated resistance, also called shunt, which determines that the cell is operating at a point near to the I_{SC} with a reduced voltage drop in comparison with the open-circuit voltage.

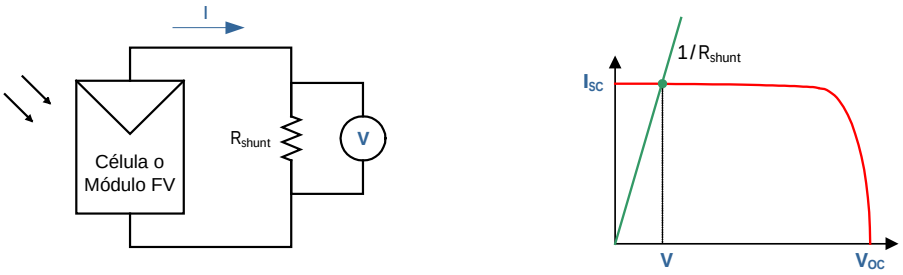

Fig. 5: Set-up to measure I_{SC} and use it as a solar irradiance sensor [22].

2.2.2 V_{OC} measurement as temperature sensor

From Eq. III, we can measure the V_{OC} of the cell and obtain the 'equivalent cell temperature', which corresponds to operating cell temperature. This is called the 'Equivalent Cell Temperature Method' and it is described in the international standard IEC 60904-5, 'Determination of the equivalent cell temperature (ECT) of photovoltaic (PV) devices by the open-circuit voltage method' [23]. By measuring the V_{OC} of the cell (Fig. 6), and knowing the cell parameters at standard conditions, the open-circuit voltage temperature coefficient at different irradiance conditions, and the current irradiance, we can calculate the equivalent cell temperature (Eq. VII):

$$T = T^* + \frac{1}{\beta}\left(V_{OC} - V^*_{OC} + \frac{mkT}{q} ln \frac{G^*}{G}\right) \qquad \textit{Eq. VII}$$

Under similar irradiance conditions, we can simplify to:

$$T = T^* + \frac{1}{\beta}(V_{OC} - V^*_{OC}) \qquad \textit{Eq. VIII}$$

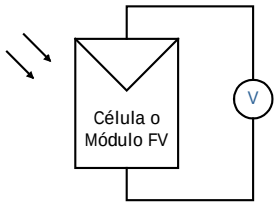

Fig. 6: Set-up to measure V_{OC} and use it as a cell temperature sensor [22].

2.3 Design requirements from solar water technologies

The three solar water technologies studied in this project in need of a low-cost sensor are SODIS, water pasteurization and natural UV photocatalytic systems.

2.3.1 SODIS

SODIS uses plastic bottles under the sun for an established number of sunshine hours, 6h if it is a sunny day and between 2-3 days if it is cloudy. These 6h of exposure to sunlight correspond approximately to a dose of 2000kJ/m^2 of UVA, considering hours of mid-latitude European midday sunshine [24]. So the PV sensor would need to measure either the number of sunshine hours, which is the main parameter that SODIS uses for clean/no clean decision, or the UV irradiation received by the bottle.

A solar cell external to the system could measure irradiance from the PV cell short-circuit current and then calculate the total number of sunshine hours. Sunshine duration has been traditionally calculated from pyrheliometers or pyranometers measuring direct irradiance or global irradiance, with dedicated algorithms established by the World Metereological Organisation (WMO) [25]. But a solar cell also measures irradiance, so it could also estimate sunshine hours. The next chapter is dedicated to study the accuracy of using a solar cell to measure sunshine duration in comparison with the already defined methods using pyrheliometers and pyranometers.

As the SODIS process use UV irradiance in their water purification process, the ideal sensor would be a dedicated UV sensor, but they are not affordable at the moment for this type of low-cost applications, with costs starting from 70€ up to 250€ per sensor or more [26]. There are some studies in the literature trying to estimate UV irradiance from

other parameters such as global irradiance, but the models usually requires additional parameters such as the ozone or the nitrogen dioxide content column [27], so they are not so easy to implement for different locations, as the UV content depends heavily on the climatic characteristics of the place. If ***we could find a method to measure UV directly from a solar cell***, such as using optical filters, a low-cost UV sensor based on solar cells could be suitable. In chapter 4 we explore this possibility when designing the clean water PV sensor.

Finally, as we can measure the global solar irradiance, if it could be done with sufficient accuracy, ***we could use the solar irradiance itself as a new parameter*** to decide when the water is clean, measuring directly the solar energy received by the water in the bottle. Regarding other specific design requirements, a sensor measuring directly sunshine hours would be an external sensor to the bottle, with the only specifications of being flat, calibrated, reliable and durable. Additionally, a second PV sensor could be integrated under the bottle, measuring the irradiance through the bottle and estimating the water temperature. In this case, the sensor under the bottle should be of a size that fits the round bottle so the optical losses are minimized (such as small, thin, flexible or elongate solar cells), and with a good thermal contact with the bottle to optimise the water temperature estimation.

2.3.2 Solar water pasteurization

Water pasteurization systems on the other hand need to know the water temperature to verify if the pasteurization temperature was reached, and for how long was the water at pasteurization temperature. So the information required is the water temperature and time at each water temperature. The most obvious sensor is to use a ***thermocouple that is prepared for liquid immersion***. In the past, these thermocouples were expensive for this type of applications in developing countries, but we will review their current cost now and compare with the PV sensor proposed. The clean water PV sensor would ***estimate the water temperature from the solar cell temperature*** by measuring the cell open-circuit voltage. The sensor should be located on top/side of the container (which in solar water pasteurization systems is black/dark) where the solar cell is in good thermal contact with the container and receiving the same solar irradiance of the container. Another requirement would be to design the sensor of a size that is sufficient to measure accurately but without

shading too much the container. If we shade the container with a large sensor, the performance of the process will be reduced as the solar irradiance reaching the water is lower.

2.3.3 Natural UV photocatalysis

Finally, natural UV photocatalytic systems will need to monitor the UV irradiance falling into the reactor and additionally, the water temperature. Ideally, a low-cost UV sensor as for the SODIS process would be required, so the adopted solution could be similar, using ***the solar cell to measure directly UV***, or ***using the global irradiance as the main parameter***. The cell could also estimate the water temperature from its open- circuit voltage.

An external PV sensor could monitor the global irradiance and estimate the water temperature if placed appropriately on top. Another option would be to place it underneath the water flow, and measure the irradiance through the system and therefore possible changes in the water transmittance related to the water pollutants concentration [13]. Regarding other design aspects, if the sensor is external it should adapt to the reactor shape and size, and if the sensor is place underneath, consider designing sensors completely adapted to the system that can circulate water directly on top of them [13].

2.3.4 Design requirements summary

Table I summarises the design requirements from the solar water technologies for a clean water PV sensor:

a) *Information requirements*: number of sunshine hours and/or UV irradiance for SODIS, water temperature and time for solar water pasteurization, and UV irradiance falling into the reactor for natural UV photocatalysis.

b) *Other design requirements*: external sensors flat, calibrated, reliable and durable, sensors underneath the bottle/reactor with size that fits the system shape, good thermal contact with the surfaces, small size for the water pasteurization systems to avoid shading.

Table I: Design requirements from the solar water technologies for a clean water PV sensor, including information requirements and other design requirements.

Solar water technology	Information required	Other design requirements
SODIS	Number of sunshine hours UV irradiance	Flat, calibrated, reliable, durable, good thermal contact Additionally if second sensor underneath bottle: Size fitting bottle shape
Water pasteurization	Water temperature & Time at each water temperature	Flat, calibrated, reliable, durable, good thermal contact Small size to avoid shading
Natural UV photocatalysis	UV Irradiance	Flat, calibrated, reliable, durable, good thermal contact Additionally if second sensor underneath reactor: Size fitting reactor shape

As stated previously, ***a solar cell could meet these information requirements*** as follows:

a) *Sunshine hours*: Measuring solar irradiance from I_{SC} and then estimating sunshine hours.
b) *UV irradiance*: Measuring directly UV irradiance from I_{SC} by using low-cost optical filters.
c) *Water temperature*: Measuring equivalent cell temperature from V_{OC} and estimating water temperature.

In the next chapter we study the use of a solar cell to measure sunshine hours from the algorithms established by the WMO, and in chapter 4 we explore the possibility of using low-cost optical filters to design a UV sensor using solar cells, as well as the estimation of water temperature from cell temperature. In the latter chapter, we also present the design of the clean water PV sensor itself.

3. ESTIMATION OF SUNSHINE DURATION FROM THE GLOBAL IRRADIANCE MEASURED BY A PV SILICON SOLAR CELL

This chapter is dedicated to the estimation of sunshine duration using photovoltaic solar cells instead of the conventional pyranometer or pyrheliometers, which result more expensive and therefore not suitable for water application technologies in developing regions. We will introduce first the need of the sunshine duration for SODIS technology and the definition of sunshine duration, followed by the description of the different methods to measure and calculate it. We will calculate the sunshine duration for a specific location using the conventional sensors and then using a photovoltaic solar cell, and then we will analyse the results and study the suitability of the solar cell for this low-cost measurement of sunshine duration.

3.1 Introduction

The definition of sunshine duration is given by the World Metereological Organisation (WMO) [25] as the number of hours for which the direct solar irradiance is above 120W/m^2. This type of measurement is often used in solar water purification processes such as SODIS (Solar Disinfection), which uses plastic bottles exposed to the sun to purify water in developing countries. SODIS establishes that for a sunny day, 6h of sunshine is sufficient to treat the water and make it safe to drink. If the day is cloudy, the time required for the water purification increases to 2-3days. Therefore, a low-cost sensor capable of estimating the sunshine hours would be suitable for SODIS water treatment and would improve its spread in developing areas.

In this project we aim for a low-cost clean water sensor based on photovoltaic cells, so the ***objective*** of this chapter is ***to study if we can use a PV silicon solar reference cell to measure sunshine duration for low cost solar water purification applications***. We will use the different algorithms proposed by the WMO that calculate sunshine duration from data such as direct irradiance, global irradiance and diffuse irradiance.

We will use the algorithms that use only global irradiance from a pyranometer, and apply them for the case of data of global irradiance that come from a PV silicon solar reference cell, and then compare the result with the result from data from a single

pyranometer and from the pyrheliometer. We will be able to see the correlation between the data from the cell and the data from the pyranometer, the possible limitations and possible correction factors, and then conclude if the cell is suitable or not and in which conditions.

3.2 Sunshine duration measurement

There are different methods to determine the sunshine duration according to the WMO [25], including the direct measurement with the Campbell-Stokes recorder, the pyrheliometric method using direct irradiance from a pyrheliometer, or pyranometric algorithms using the global irradiance from a pyranometer. There are also additional pyranometric methods not adopted yet by the WMO but that are well-reviewed in the literature aiming to improve the pyranometric algorithm used by the WMO [28, 29, 30].

3.2.1 Campbell-Stokes sunshine recorder

This instrument was introduced in 1880, and it is composed by a glass sphere that concentrates the sun radiation beam onto a graduated paper card that burns according to a sunshine intensity threshold (Fig. 7). The sunshine duration is read from the total burn length. The WMO considers that it does not provide accurate data as the burns are subjected to errors caused by possible mounting adjustments problems and to the fact that the burns depend heavily on the card temperature and humidity.

(a) (b)

Fig. 7: a) Campbell-Stokes recorder showing the glass sphere, the support and the position of the card [31]; b) Card after a day of measurement, showing the burnt parts used to calculate sunshine duration [32].

3.2.2 Pyrheliometric method

The sunshine duration definition given by the WMO as '*the number of hours for which the direct solar irradiance is above 120W/m^2*' requires a more accurate method than the Campbell-Stokes recorder. On this regard, direct solar irradiance is measured by a pyrheliometer mounted on a sun tracker (normal to the sun), monitored automatically (Fig. 8). A pyrheliometer measures only the direct solar irradiance by using a thermopile with a broadband spectral response (entire spectrum) and with a narrowed aperture. It requires continuous sun tracking. The sunshine duration is then obtained by comparing the direct solar irradiance measured by the pyrheliometer with the threshold of 120W/m^2 and integrating during the day length. In summary, the data required and the sunshine duration calculation using the pyrheliometric method are:

- *Data*: Direct solar irradiance from a pyrheliometer with a resolution of 1 minute.
- *Sunshine duration*: Period composed by the sub-periods in which the direct solar irradiance is above 120W/m^2. The sub-period is 1min.

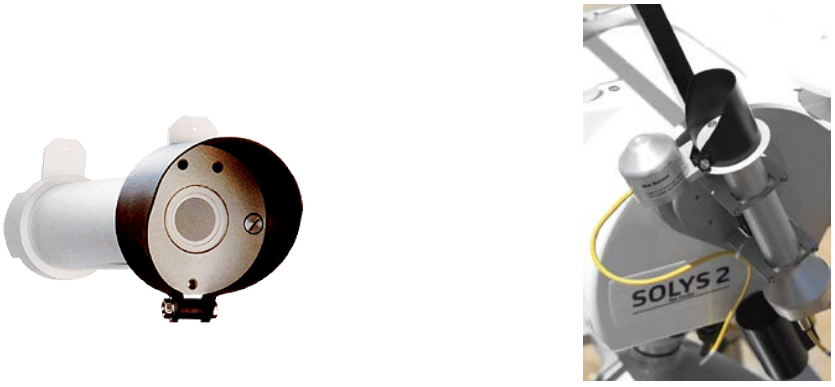

(a) (b)

Fig. 8: Single pyrheliometer [22] (a) and pyrheliometer mounted in a suntracker (b) to measure automatically direct solar irradiance, from Kipp and Zonen [33].

3.2.3 Pyranometric methods

Other methods used by the WMO are based in the global radiation measurement by using a pyranometer. A pyranometer consists of a thermopile with a broadband spectral response, same as the pyrheliometer, but this time the aperture is not narrowed but widened using a semispheric glass dome (Fig. 9a). If we use a shading ring or a shading ball to block the direct radiation reaching the pyranometer, we obtain the diffuse radiation. The

shading ball requires sun tracking (Fig. 9b) and the shading ring does not but weekly elevation adjustment.

(a) (b)

Fig. 9: a) Pyranometer; b) Sun tracker including a pyrheliometer measuring direct radiation, two pyranometers measuring global, and a third pyranometer with the shading ball measuring diffuse radiation [33].

The relationship between direct solar radiation, global and diffuse is:

$$I \cos\theta = G - D \qquad Eq.\ IX$$

where $I$is the direct solar radiation on the normal plane, $I \cos\theta$ is the horizontal component of the direct solar radiation, θ is the solar zenith angle, G is the global solar horizontal radiation, and D is the diffuse solar horizontal radiation.

If there are ***two pyranometers*** available, one for global solar radiation and one for diffuse solar radiation then the WMO method is to calculate the direct solar radiation component (by using the relationship given in Eq. IX) and then apply the threshold of 120W/m^2. Therefore, this method uses:

- *Data*: Global solar irradiance from a pyranometer and Diffuse solar irradiance from a pyranometer with shading ring or shading ball and tracker, with 1-min resolution.
- *Sunshine duration*: Period composed by the 1-min sub-periods in which the direct solar irradiance, calculated as $I = (G - D)/\cos\theta$, is above 120W/m^2.

But if there is only ***one pyranometer*** available, measuring global horizontal solar radiation, then the sunshine duration calculation is not so straightforward. Several algorithms have been proposed by different authors [28, 29, 30] using the global horizontal and other common parameters, such as the latitude, longitude, cloud cover, turbidity,

temperature, etc. We will discuss some of these algorithms in the next sub-section. From all of them, the WMO currently uses the Slob and Monna algorithm. This algorithm was developed by Slob and Monna in 1991. It uses the mean, minimum and maximum of global solar radiation in a 10 minute interval. It is based in an estimation of the direct (Eq. X) and diffuse (Eq.XI) components for cloudless conditions, which depends on the Linke turbidity factor T_L (related to the trace gases and aerosols in the atmosphere), the solar constant ($I_0 = 1367\ W/m^2$) and the cosine of the solar zenith angle ($\mu_0 = cos\ \theta$). These estimations are based on a three year dataset in the Netherlands (1986-1989) and are as follows:

$$I = I_0 \exp\left(-T_L/(0.9 + 9.4\mu_0)\right) \qquad \textit{Eq. X}$$

where I is the parameterised estimation of direct solar irradiance for cloudless conditions, I_0 is the solar constant, T_L is the turbidity factor and μ_0 is the cosine of the solar zenith angle.

$$D/G_0 = \begin{cases} 0.2 + \mu_0/3 & \text{for } 0.1 \leq \mu_0 \leq 0.3 \\ 0.3 & \text{for } \mu_0 \geq 0.3 \end{cases} \qquad \textit{Eq. XI}$$

where D is the parameterised estimation of diffuse solar irradiance for cloudless conditions and G_0 is the horizontal radiation in the atmosphere ($G_0 = I_0\mu_0$).

The algorithm compares the measured global solar irradiance G with the lower limit for cloudless conditions, which is $I\mu_0 + D$. This comparison is conducted with all the values normalized by G_0. Fractional values of sunshine f are then calculated for 10-min intervals (0 – no sunshine at all, 1 – only sunshine, between 0 and 1 – partly sunshine, partly clouded), and sunshine duration SD is obtained by multiplying f by 10. The complete algorithm is shown in Fig. 10.

In summary, the pyranometric method used by the WMO with only a single pyranometer measuring global radiation uses:

- *Data*: Global horizontal irradiance from a pyranometer.
- *Sunshine duration estimation*: Slob and Monna algorithm.

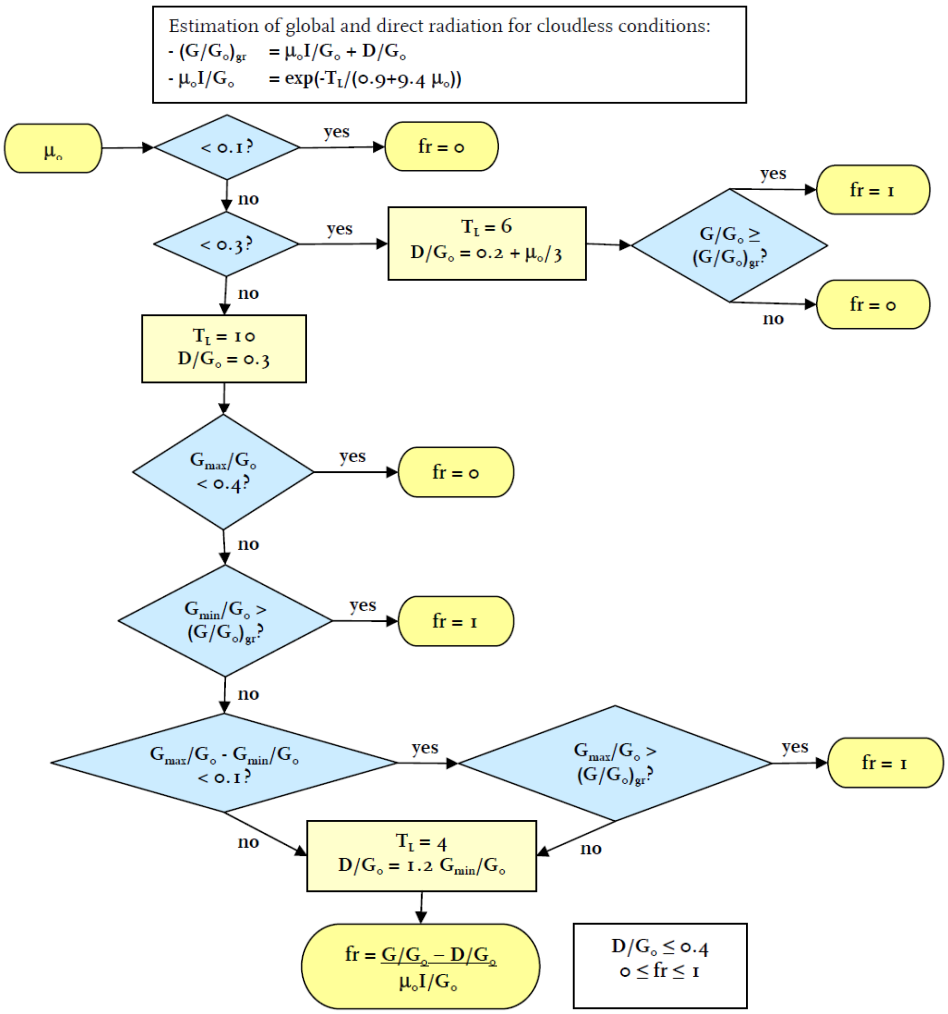

Fig. 10: The Slob and Monna algorithm to estimate sunshine duration from one-single pyranometer readings of global horizontal radiation. Fractional values of sunshine f are calculated for 10-min intervals, comparing with estimated values of direct and diffuse radiation for cloudless conditions [34].

3.2.4 Other pyranometric methods

As we mentioned earlier, there are other pyranometric methods developed by researchers at different metereological agencies from different countries. One of the most successful and accepted algorithms is the ***Hinssen-Knap algorithm***, developed by Hinssen and Knap in 2006 by adjusting the Slob algorithm [28, 34]. The improved algorithm directly relates sunshine duration to 10-minute mean measurements of global irradiance (Fig. 11). There is a lower limit l_i for G/G_0, and below it there is no sunshine ($f = 0$), and upper limit u_i , and above it there is full sunshine ($f = 1$). Between the limits, the sunshine duration is a linear function related to the normalised global irradiance. The algorithm has two different intervals depending on the sun elevation angle ($\mu_0 < 0.3$; $\mu_0 \geq 0.3$). The

optimum values for l_1, u_1, l_2 and u_2 need to be established by calculating the pyrheliometric fractional values of SD for 10-min intervals and representing vs. the normalised global irradiance G/G_0. For the dataset and location considered under their study, which corresponds to 1-year data at the station of Cabauw (Netherlands, 51.97ºN and 4.93ºE), the optimum values were of $l_1 = 0.4, u_1 = 0.5,\ l_2 = 0.45$ and $u_2 = 0.6$. These values should be calculated for new locations, especially when in different climatic areas.

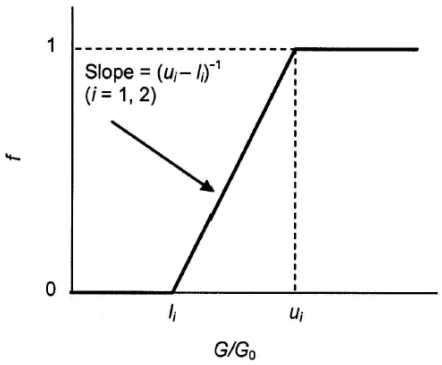

$$
\begin{aligned}
\mu_0 < 0.3: \quad & G/G_0 < l_1 && \rightarrow \quad f = 0 \\
& l_1 \le G/G_0 < u_1 && \rightarrow \quad f = (G/G_0 - l_1)(u_1 - l_1)^{-1} \\
& G/G_0 \ge u_1 && \rightarrow \quad f = 1 \\
\mu_0 \ge 0.3: \quad & G/G_0 < l_2 && \rightarrow \quad f = 0 \\
& l_2 \le G/G_0 < u_2 && \rightarrow \quad f = (G/G_0 - l_2)(u_2 - l_2)^{-1} \\
& G/G_0 \ge u_2 && \rightarrow \quad f = 1.
\end{aligned}
$$

Fig. 11: The Hinssen-Knap correlation algorithm, showing the linear relationship of sunshine duration with the mean global solar irradiance and the limits established for two different intervals depending on the sun elevation angle [28].

In a recent report from 2011, F. Massen [30] has reviewed several pyranometric algorithms, including the Olivieri algorithm, the Slob and Monna, the Hinssen-Knap, the Louche ½ the Campbell and the Glover. He uses the Hinssen-Knap as the reference algorithm for comparison, and concludes that the other most accurate and easy to use for calculating the sunshine duration in accordance with the WMO definition is the Olivieri one. In 2012, Vuerich et al. [29] also presented an evaluation of several pyranometric algorithms. The algorithm included the Slob and Monna one and the Olivieri, among others. They also concluded that the algorithm providing better results, with less uncertainty, was the ***Olivieri algorithm***. This algorithm was developed at the Météo France in 1998 [29], and it compares the global irradiance to a threshold value that is a function of F, which represents a fraction of the global irradiance in clear sky in average conditions of turbidity (Fig. 12). The coefficients A and B are specific for each location. Météo France calculated an empirical table including the coefficients for different location latitudes.

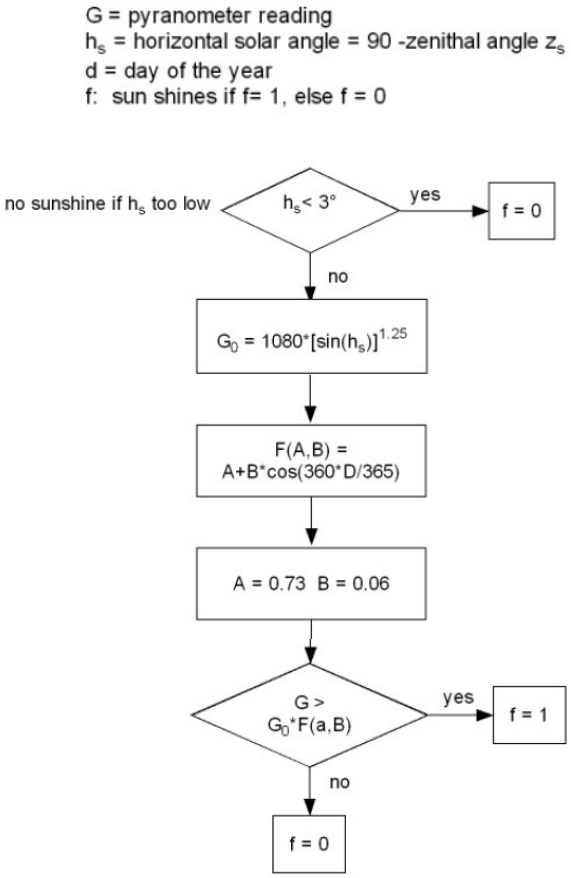

Fig. 12: The Olivieri correlation algorithm [30], estimating sunshine duration on 1-min basis comparison of global horizontal solar radiation with a threshold function of a fraction F of the global irradiance in clear sky in average conditions. Values of A and B are specific for each location, for this case they correspond to a latitude of 44ºN.

In summary, we have presented a description of the main methods to calculate sunshine duration using different equipment: first, by means of a Campbell-Stokes recorder; second, using directly a pyrheliometer (direct radiation) and a sun tracker; third, with the pyranometric method using two pyranometers (global and diffuse radiation); and finally, using just one pyranometer measuring global, presenting three different algorithms in detail.

3.3 Estimation of SD from global solar irradiance measured by a solar cell

All the previous methods to calculate SD are very accurate but they require expensive equipment such as a pyrheliometer, a sun tracker or a pyranometer, which are affordable for a metereological weather station but not for day-to-day applications in developing countries. In our case, solar water purification systems in developing countries need low

cost sensors with an acceptable performance, so a trade-off between cost and performance must be achieved.

A solar cell could be used to measure sunshine duration at low cost as it can measure incident solar radiation according to its spectral response. But the solar cell spectral response is not broadband but limited according to the energy bandgap (till 1100nm for a silicon solar cell). The other limitation is that the spectral response is not flat as in a thermopile, but with a maximum responsivity in the near-infrared. So the output depends on the solar radiation spectrum; and the WMO does not use sunshine duration detectors based only in purely silicon photovoltaic solar cells because these spectral variations are a source of error [25]. Other limitations include the reduced field-of-view in comparison with a pyranometer and the annual degradation of a solar cell (~1% for monocrystalline silicon cells).

These limitations of photovoltaic solar cells to measure global irradiance are discussed further in the next chapter. In this section, we are going to try to quantify the effect of these spectral variations in comparison with a pyranometer and a pyrheliometer when calculating SD. The objective is to analyse if the SD calculated by a solar cell in relation to a pyranometer is well-correlated or not, and if it would be suitable for low-cost applications despiting losing performance.

3.3.1 Methodology

Using a 1-year dataset with direct solar radiation data from a pyrheliometer with sun tracker, global solar radiation from a pyranometer and global solar radiation from a calibrated silicon photovoltaic solar cell, we calculated the sunshine duration using the pyrheliometric method and three of the pyranometric methods.

The sunshine duration calculated from the pyrheliometer, SD_{Pyrh}, was used as the reference data. The three pyranometric algorithms used were the Slob and Monna, the Hinssen-Knap and the Olivieri. They were applied to the global data provided by the pyranometer, calculating sunshine durations, SD_{Slob_Pyr}, SD_{Hins_Pyr} and SD_{Oli_Pyr}. They

were also applied to the global data from the silicon photovoltaic solar cell for comparison, obtaining SD_{Slob_Si}, SD_{Hins_Si} and SD_{Oli_Si}.

As both the pyranometer and the silicon photovoltaic solar cell were at a tilted angle and not in a horizontal plane, the algorithms were corrected to compare with a tilted surface. For Slob and Monna (and so for Hinssen and Knap), the estimations of direct normal and diffuse were corrected for a tilted surface with an angle β:

$$I_\beta = I \cos \nu \qquad \textit{Eq. XII}$$

$$\cos \nu = \cos \gamma_s \cos \alpha_s \sin \beta + \sin \gamma_s \cos \beta \qquad \textit{Eq. XIII}$$

$$D_\beta = D \ \frac{1+\cos \beta}{2} \qquad \textit{Eq. XIV}$$

$$G_\beta = I_\beta + D_\beta \qquad \textit{Eq. XV}$$

where I_β is the estimated direct normal at the tilted surface; ν is the angle of incidence respect to the tilted surface; γ_s is the sun elevation angle; α_s is the solar azimuth, β is the tilt angle; D_β is the estimated diffuse radiation at the tilted surface; and G_β is the estimated global radiation at the tilted surface.

The global horizontal extraterrestrial irradiance G_0 was also substituted for the global extraterrestrial irradiance at tilted surface, $G_{0,\beta}$, using the incident angle ν, $G_{0,\beta} = I_0 \cos \nu$, for the three algorithms. Hinssen correlation optimum limits were established for the new solar radiation dataset, obtaining $l_1 = 0.1$, $u_1 = 0.8$, $l_2 = 2$ and $u_2 = 0.7$.

3.3.2 Solar radiation data

Solar radiation data correspond to the meteorological station and photovoltaic installation from the Photovoltaic Technology Group at the University of Cyprus, Nicosia, Cyprus. Latitude is 35.2º N and longitude 33.5º E. The direct normal irradiance is measured by a Kipp&Zonen CH1 pyrheliometer and the global irradiance by a

Kipp&Zonen CM29 pyranometer. The calibrated photovoltaic solar cell used as a global irradiance sensor is a monocrystalline silicon solar cell. Both the pyranometer and the calibrated cell are at a tilt angle of 27.5º. Data are sampled and stored every minute.

One-year data were used for this study, from December 2011 to November 2012. Data quality was checked in order to first eliminate those days with technical problems, such as power losses, sun-tracking issues or data acquisition irregularities. Main problems were related to the sun-tracker (67 days) and the data acquisition system of the photovoltaic solar cell (12 days). A second quality control stage consisted on a filtering to detect solar radiation data that might be erroneous, checking the physically possible limits of solar radiation and the extremely rare limits.

3.3.3 Results

In this section we will compare the sunshine durations calculated by the pyranometric methods, both for the pyranometer and the solar cell, and compare with the pyrheliometric sunshine duration. We will analyse first the overall results for each of the methods and then we will focus on the results from the photovoltaic cell, which is the objective of this study.

Table II presents a summary of the yearly totals of SD for the different methods: pyrheliometric, Slob and Monna pyranometric algorithm, Olivieri pyranometric algorithm and Hinssen pyranometric algorithm. The sunshine duration calculated by the pyrheliometer is 2171 h. The cumulative difference of the pyranometric algorithms over the year is provided, observing that the Hinssen and Knap algorithm gives the best estimation, with -145 h (-7%) and -61 h (-3%), for the pyranometer and the cell, followed by the Slob and Monna algorithm, -411 h (-19%) and -210 h (-10%), and the Olivieri algorithm, -457 h (-21%) and -372 h (-17%). All the algorithms underestimate sunshine duration over the span of a year.

On a daily mean basis, the Hinssen and Knap algorithm gives -0.4 ± 0.08 h/day (± 20%) and -0.17 ± 0.11 h/day (± 65%), the Slob and Monna algorithm provides -1.12 ± 0.05 h/day (± 4%) and -0.57 ± 0.08 h/day (± 14%); and the Olivieri algorithm gives -1.25 ± 0.06 h/day (± 5%) and -1.02 ± 0.07 h/day (± 7%). Which means that the uncertainty for the

Hinssen and Knap on a daily basis is extremely high and that the either the Slob and Monna algorithm or the Olivieri are suitable to measure sunshine duration when using the pyranometer. For the case of the solar cell, the most suitable algorithm on a daily basis is the Olivieri. The main conclusion of this analysis is that the silicon solar cell is capable of measuring sunshine duration on a daily basis with an uncertainty similar to the obtained with a pyranometer when using the Olivieri algorithm. For the other two algorithms, Hinssen and Knap and Slob and Monna, the uncertainty is considerably higher than the SD calculation from the pyranometer.

Table II: Yearly totals of SD for the different methods: pyrheliometric, Slob and Monna pyranometric algorithm, Olivieri pyranometric algorithm and Hinssen pyranometric algorithm (h/year), cumulative difference with pyrheliometric SD (h/year) and mean difference (h/day) and standard deviation (h/day).

Method	Instrument	SD (h/year)	Difference (h/year)	Mean difference (h/day)	Standard error of the mea (h/day)
Pyrheliometric	Pyrheliometer	2171	--	--	--
Slob and Monna	Pyranometer	1760	-411	-1.12	0.05
Hinssen and Knap	Pyranometer	2026	-145	-0.4	0.08
Olivieri	Pyranometer	1714	-457	-1.25	0.06
Slob and Monna	PV Si cell	1961	-210	-0.57	0.08
Hinssen and Knap	PV Si cell	2110	-61	-0.17	0.11
Olivieri	PV Si cell	1799	-372	-1.02	0.07

Fig. 13 shows the calculated daily sunshine duration of the three algorithms vs. the sunshine duration calculated by the pyrheliometer. On the left we can observe the results for the pyranometer and on the right for the Si photovoltaic cell. As discussed, the Olivieri algorithm gives the better adjustment with the pyrheliometer for the solar cell. All the algorithms underestimate the sunshine duration hours relatively to the pyrheliometric sunshine duration. For the case of Slob and Monna, this is already well-studied in the literature [28], as this algorithm starts considering sunshine when the elevation angle is above 5.7º. The Hinssen algorithm lowers this limit to 2.9º and the Olivieri to 3º. Another reason for underestimation in this particular study is due to the tilted surface of the pyranometer, which can result in receiving less light at small elevation angles at sunrise

and sunset, when the sun can be even behind the pyranometer. This is more critical even for the tilted solar cell, as it will not receive solar radiation at high azimuth solar angles. However, if the aim is to calculate sunshine duration for a particular surface tilted and positioned similarly to the silicon solar cell, and with and equivalent reduced field-of-view, it will be more accurate to use the solar cell than using the pyranometer. It is the same concept as used in photovoltaic power plants, using a calibrated solar cell of the same technology as the PV modules and in the same position to measure solar radiation gives the energy that the photovoltaic modules are able to convert into electricity ('usable energy'), and therefore, production estimations and calculations are more accurate [35].

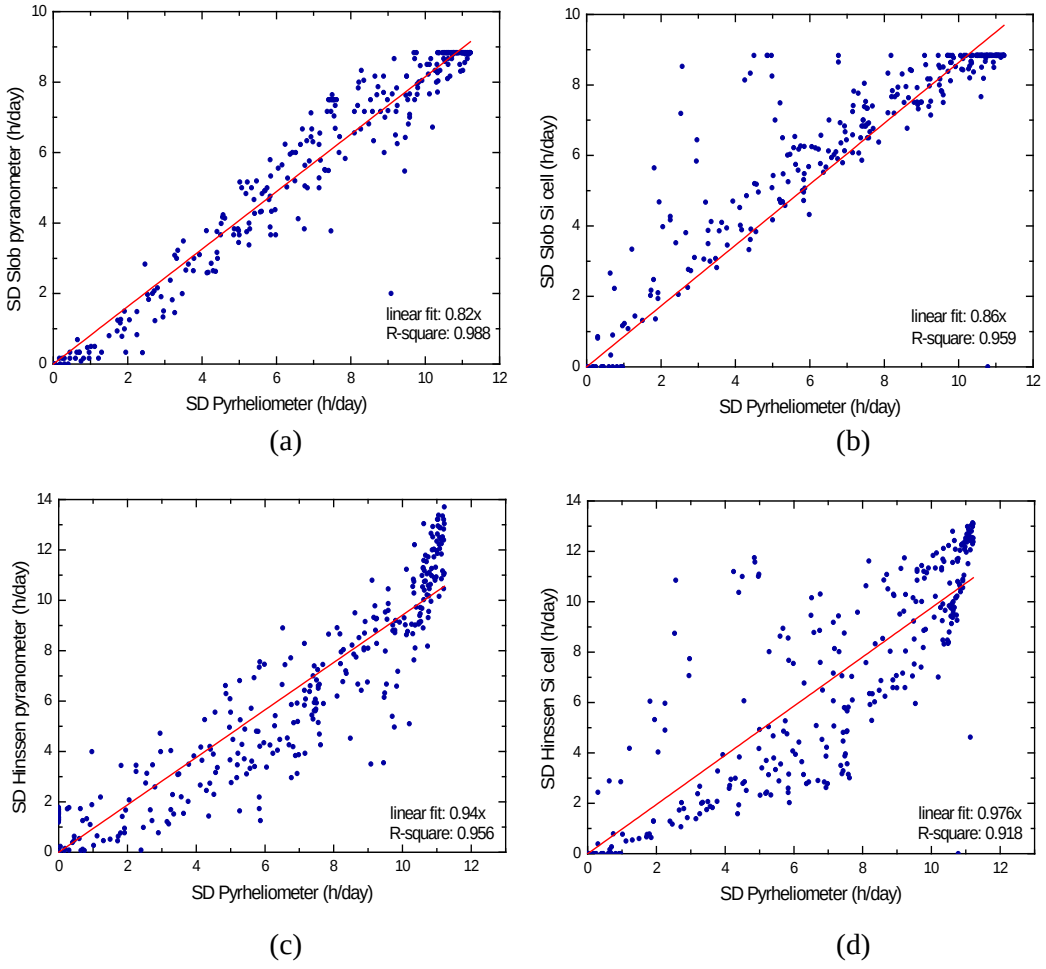

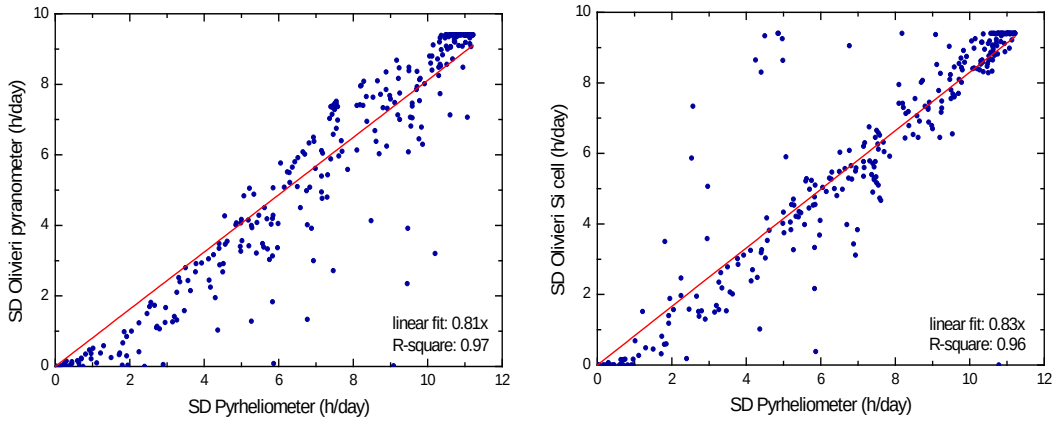

(e) (f)

Fig. 13: Daily sunshine duration calculated with the three algorithms (Slob, Hinssen and Olivieri) vs. the sunshine duration calculated by the pyrheliomter for both the pyranometer (a,c,e) and the silicon solar cell (b,d,f), showing the correlation between them and the linear fitting.

Fig. 14a gives the frequency distribution for the difference between the daily SD calculated by the solar cell using the Olivieri algorithm and the pyrheliometer. We can see how the SD is underestimated as most of the values are below zero. The daily mean difference is -1.02 h and the standard deviation is of 1.4 h. Fig. 14b shows the cumulative probability of the daily difference, with 95% of the values below +0.25h of difference.

Fig. 15 shows the box plot of the differences between the daily SD calculated for the three algorithms using the solar cell and the SD calculated from the pyrheliometer. It shows again how the Olivieri algorithm is the most suitable for the measurement of sunshine duration with a photovoltaic solar cell.

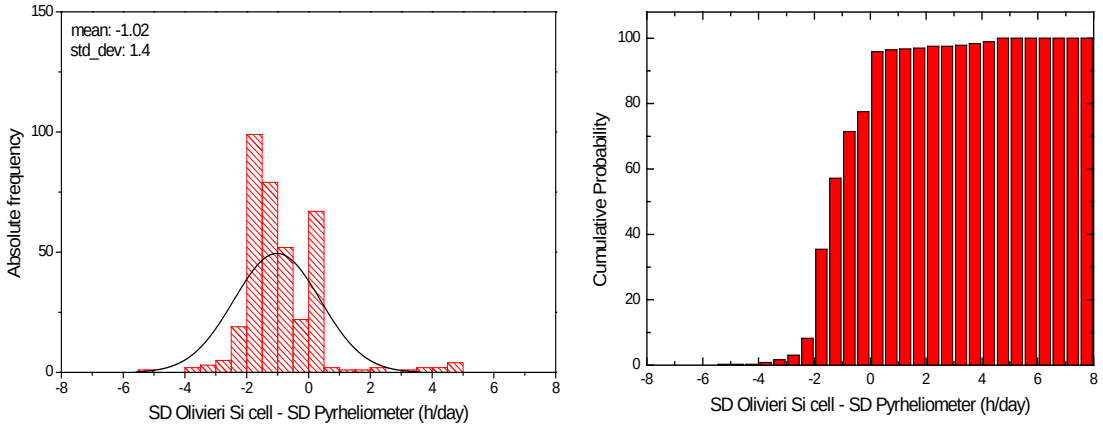

(a) (b)

Fig. 14: a) Absolute frequency of the difference between daily SD calculated with the Olivieri algorithm and the solar cell and the SD calculated with the pyrheliometer (h/day);
b) Cumulative probability of SD Olivieri Si cell – SD Pyrheliometer (h/day).

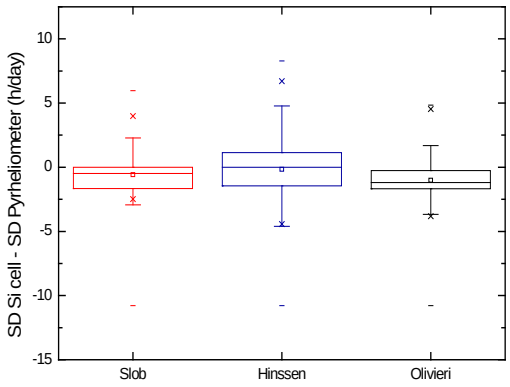

Fig. 15: Box plot of SD Si cell – SD Pyrheliometer (h/day) for the three algorithms, Slob, Hinssen and Olivieri, showing that the Olivieri algorithm gives the better adjustment for measuring SD with a photovoltaic solar cell.

Finally, if we analyse the sunshine duration calculated by the solar cell seasonally, separating into Spring (April-May-June), Summer (July-August-September), Autumm (October-November-December) and Winter (January-February-March), we can observe that the Slob algorithm underperforms in the summer months, is similar in spring and autumm and improves in winter. This agrees with previous studies and analysis [28]. On the other hand, the Hinssen algorithm overestimates in spring and Summer and underestimates substantially in autumm and winter, with high variation in adjustment. Finally, the Olivieri algorithm underestimates over the four seasons, but it is more affected in the summer and winter months.

The tilted position of the cell, as discussed earlier, affects the performance of the different algorithms, as well as the definition of the codes for the different algorithms. It is important to observe that the algorithms were developed mostly in the Netherlands and Northern Europe, with different climatic conditions than those from the south, corresponding to the solar radiation data for this study. Previous studies worked with a yearly number of sunshine hours of about 1400, and the location in this study was working with about 2200. It is also expected that turbidity values vary considerably from one location to another, so this could affect also the performance of the algorithms.

Table III: Seasonal pyrheliometric sunshine duration and differences between the sunshine durations calculated by the three pyranometric algorithms using the solar cell. Autumm months have less total hours due to the reduced number of quality-data days due to technical problems.

	Spring	Summer	Autumm	Winter
SD Pyrheliometric (h)	619	737	272	544
SD Slob Si cell -SD Pyrh (h)	-30	-132	-33	-17
SD Hinssen Si cell -SD Pyrh (h)	165	25	-119	-133
SD Olivieri Si cell - SD Pyrh (h)	-49	-124	-90	-109

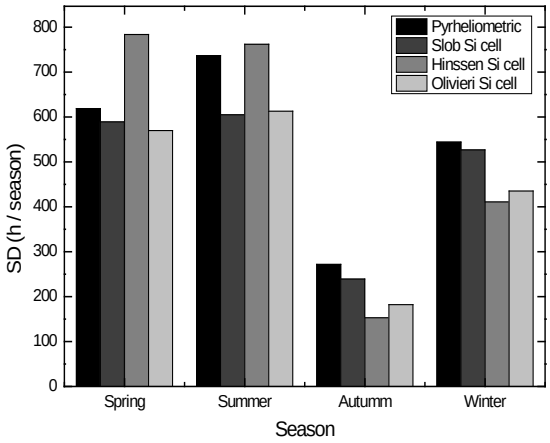

Fig. 16: Seasonal sunshine duration calculated by the pyrheliometer and the three pyranometric algorithms using the solar cell: Slob, Hinssen and Olivieri.

3.4 Summary and conclusions

The objective of this chapter was to study if we could use a PV silicon solar reference cell to measure sunshine duration for low cost solar water purification applications. A comparison between the standard methods defined by the WMO, using a pyrheliometer to measure sunshine duration, and different algorithms when using a single pyranometer, has been conducted including the calculation of sunshine duration using a solar cell and the pyranometric algorithms.

The evaluation was performed using solar radiation data from the meteorological station and photovoltaic installation from the Photovoltaic Technology Group at the University of Cyprus, Nicosia, Cyprus, for the period December 2011 to November 2012. Three pyranometric algorithms were used: the Slob and Monna, the Hinssen and Knap and the Olivieri method. The algorithms were adapted to the tilted pyranometer and calibrated

photovoltaic silicon solar cell from Cyprus. The pyrheliometric method gave an annual sunshine duration of 2171h.The pyranometric methods provided annual sunshine durations differences of -145 h (-7%) and -61 h (-3%) for the Hinssen and Knap algorithm (pyranometer and cell); of -411 h (-19%) and -210 h (-10%) for the Slob and Monna; and of -457 h (-21%) and -372 h (-17%) for the Olivieri. All the algorithms underestimate sunshine duration over the span of a year and the results between the pyranometer and the solar cell were comparable.

On a daily difference mean basis, the Hinssen and Knap algorithm had an excessive dispersion and uncertainty in the SD values, (-0.4 ± 0.08 h/day (± 20%) and -0.17 ± 0.11 h/day (± 65%)). The Slob and Monna had less uncertainty but still high for the solar cell results (-1.12 ± 0.05 h/day (± 4%) for the pyranometer and -0.57 ± 0.08 h/day (± 14%) for the cell). Finally, the Olivieri algorithm gave a daily mean difference with the pyrheliometric method of -1.25 ± 0.06 h/day (± 5%) for the pyranometer and of -1.02 ± 0.07 h/day (± 7%) for the solar cell, both acceptable results and very similar between them.

The main conclusion is that the silicon solar cell is capable of measuring sunshine duration on a daily basis with an uncertainty similar to the obtained with a pyranometer when using the Olivieri algorithm. It can measure sunshine duration on a daily basis with an uncertainty of 1.4h/day, which is sufficient for the low-cost solar water applications, as we can overexposed the device to the sun to reduce this uncertainty. Again, this difference and uncertainty value is relative to a pyrheliometer, and although it underestimates, it might be more useful as it will give an indication of the real sunshine hours that a device with the same characteristics and limitations (same position, similar reduced field-of-view) as the solar cell is exposed to.

4. DESIGN AND MANUFACTURING OF A CLEAN WATER PV SENSOR

In this chapter, we will design a generic clean water sensor based in photovoltaic solar cells. A review of previous sensors based on PV cells for measuring irradiance and cell temperature for PV plants will be conducted, prior to the design of the clean water PV sensor of this project. Finally, the manufacturing process and the initial calibration of the sensor will be described.

4.1 Previous PV sensors designs for measuring irradiance and temperature for PV plants

Sensors based in calibrated solar cells have been widely used in photovoltaics to monitor the performance of PV plants. These solar cells are called 'reference cells' and their characteristics and calibration and are defined in the international standard IEC 60904 [36]. From their generated photocurrent, which depends on the number of photons and their spectral distribution, they calculate the solar irradiance. But the measured solar irradiance depends on the spectral response of the cell, which extends from the UV to the NIR, so it does not measure the broadband solar irradiance as a pyranometer does (Fig. 17). So they cannot be used as radiometers to measure the total weather data accurately, but they can be used to measure the solar irradiance that is available to a PV module for energy conversion, as both the reference cell and the PV module have the same spectral response [37].

Meybray et al. from NREL have recently reviewed the difference between using pyranometers and reference cells when monitoring PV plants performance [37], giving a comparison between pyranometers and reference cells when they are used for measuring the efficiency of PV at reference conditions and when they are used as radiometers. When used for measuring the efficiency of PV modules, the reference cell matches the spectral response of the PV module, so it is more accurate. The pyranometer measures the broadband spectrum (UV to FIR) and the response needs to be corrected for PV. On the contrary, a pyranometer is ideal to measure the weather (entire spectrum) but the reference cell will be consider insufficient (only UV to NIR). Medbray et al. also compare other parameters such as the angle of incidence effect, temperature response and time response. Finally, they suggest, as other authors in the literature, such as Haeberlin et al. [38] or

Dunn et al. [39], the use of reference cells instead of pyranometers [40] to monitor PV plants performance because they are a matched reference device that provides a better and more realistic estimation of the expected energy output of a PV plant.

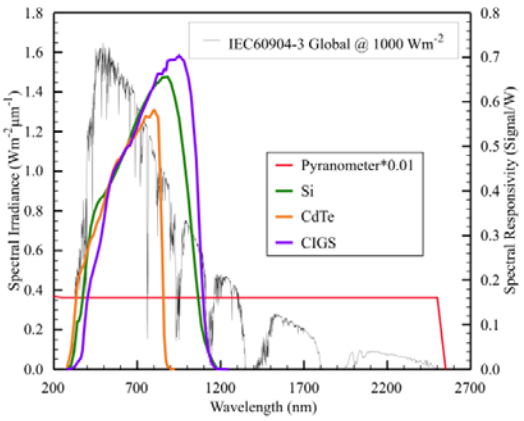

Fig. 17: Spectral response of a pyranometer (in red) showing the broadband response in comparison with the spectral response of several photovoltaic solar cells technologies that can be used as reference cells, including silicon (in green), CdTe and CIGS [37].

An example of a well-developed sensor based in reference cells is the ESTI sensor, designed at developed at the European Solar Test Installation (Joint Research Centre - JRC, Ispra, Italy) to monitor PV plants within the 1994 German program 'A Thousands Roofs' [41]. It consists of a monocrystalline solar cell encapsulated in glass/EVA/ polyester-aluminium-tedlar. The cell is cut in two, with one half used to measure I_{SC} and the other half to measure V_{OC}. The electronic system is laminated inside the sensor, with a final size of 140mm x 140mm. The ESTI sensor is then calibrated for irradiance and cell temperature, obtaining a final measurement accuracy of ±2% for irradiance and ±2ºC for cell temperature. Fig. 18 shows an image of a recent Suntech ESTI type reference cell calibrated by PV Evolution Labs.

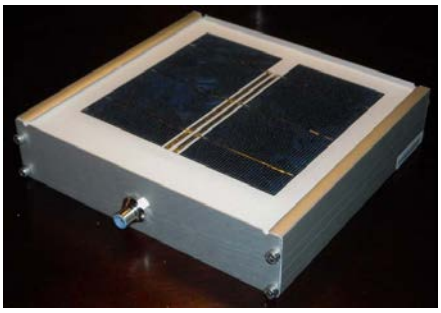

Fig. 18: Suntech ESTI type reference cell calibrated by PV evolution labs, showing the two halves of the silicon solar reference cell (in this case multicrystalline) used as a sensor, encapsulated using the same materials as for a PV module [37].

4.2 Clean water PV sensor design

A photovoltaic solar cell can be used to measure global irradiance as stated previously, with a spectral response that includes UV, Vis and NIR. We can measure the global irradiance from the cell and then estimate the sunshine duration as studied in the previous chapter, which is the main parameter used in SODIS as a criteria of clean water. On the other hand, we would like to measure directly the UV irradiance, but the cell measures UV, Vis and NIR. One possibility would be to use an optical filter that blocks all the light except the UV, but these specific filters are too expensive for this type of applications.

A solution to this problem of ***measuring directly UV with a solar cell is to use two solar cells and a low-cost UV filter for one of the cells, which blocks just the UV part of the spectrum***. The first cell would measure the global solar irradiance (comprising UV, Vis and NIR), and the second cell would be under the low-cost UV filter, measuring the global solar irradiance except the UV (Vis and NIR). ***By differentiating the response of the two cells, we would have just the UV component of irradiance***. This would be a low-cost solution since the solar cell is currently affordable due to the booming of the PV industry and the plummeting of silicon technologies costs, with a cost of 0.1€ per cell or less depending on the technology, and the UV filter could be an inexpensive UV filter from photography or from the glass protection and safety films industry.

Considering the design requirements described in chapter 2, the previous PV sensors developed for PV plants performance monitoring and the solution adopted to measure UV irradiance directly with two solar cells, we are proposing a clean water PV sensor design that follows the ESTI sensor approach from the JRC. The sensor is composed by a set of two basic units, each basic unit comprising two single PV cells of the same technology, encapsulated in the initial design using the same materials as for a PV module. Each sensor includes two of these units: the first one as a reference unit, placed always external to the solar water treatment system, and the second as water test unit, placed in different locations depending on the solar disinfection technology (Fig. 19):

a) The *reference unit* will comprise a first cell measuring I_{SC} and therefore global irradiance; and a second cell will be under an UV filter, measuring I_{SC} and therefore global irradiance except UV. With this reference unit we can measure global irradiance, sunshine hours and UV irradiance.

b) The *water test unit* will include a third cell measuring I_{SC} and therefore global irradiance through or on the water (depending on where we place the unit), and a fourth cell measuring V_{OC}, and therefore cell temperature and an estimation of water temperature.

For the case of SODIS the water unit would be located under the bottle, and for solar water pasteurization on top of the container. In summary, the sensor is composed by 4 cells, 2 directly under the sun as a reference (so we can normalise) and 2 integrated in the solar water technology.

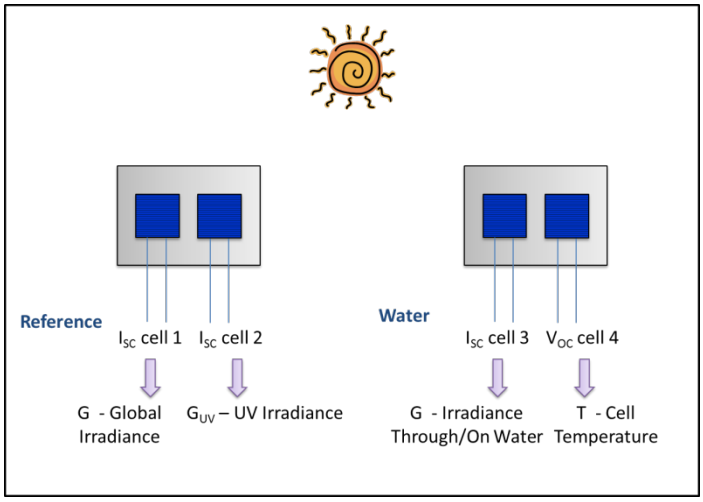

Fig. 19: Clean water PV sensor design including one unit as a reference, measuring solar irradiance and UV irradiance, and another unit for the water, measuring irradiance through/on the water and water temperature.

The 4 cells from the clean water PV sensor will provide four basic parameters based on the short-circuit current and open-circuit voltage of the cells:

- *Reference unit*:
  - I_{SC} from cell 1 → Solar irradiance.
  - I_{SC} from cell 2 → Solar irradiance except the UV.
- *Water unit*:
  - I_{SC} from cell 3→ Irradiance through/on the water.
  - V_{OC} from cell 4 → Cell 4 temperature and water temperature estimation.

Using the solar cell characteristic equations from chapter 2 we obtain the different parameters:

a) Solar Irradiance - G

From the reference unit short-circuit current of cell 1 $I_{SC,Cell_1}$, we obtain directly the solar irradiance G in W/m^2:

$$G = G^* \frac{I_{SC,Cell_1}}{I^*_{SC,Cell_1}} \qquad \textit{Eq. XVI}$$

where

$G^* = 1000W/m^2$, the irradiance corresponding to standard conditions, and

$I^*_{SC,Cell_1}$ is the cell short-circuit current in A at standard conditions of $1000W/m^2$, obtained when we calibrate the cell.

b) UV Irradiance - G_{UV}

From the reference unit short-circuit current of cell 2, $I_{SC,Cell_2}$(Vis, NIR), and the short-circuit current of cell 1, $I_{SC,Cell_1}$ (UV, Vis, NIR), we calculate the UV solar irradiance G_{UV} in W/m^2:

$$G_{UV} = G - G^* \frac{I_{SC,Cell_2}}{I^*_{SC,Cell_2}} \qquad \textit{Eq. XVII}$$

where

G is the solar irradiance, obtained by the cell 1 in the reference unit.

$G^* = 1000W/m^2$, the irradiance corresponding to standard conditions, and

$I^*_{SC,Cell_2}$ is the cell short-circuit current in A at standard conditions of $1000W/m^2$, obtained when we calibrate the cell.

This calculation assumes that the UV blocking filter is ideal and that it rejects only all the UV and transmits the visible and infra-red light components. We will review this and study the validity of this assumption, using it as an adequate estimation for this particular application in further chapters (Chapter 5).

c) Solar Irradiance through the water or on the water - G_{water}

From the water unit short-circuit current of cell 3, $I_{SC,Cell_3}$, we obtain directly the solar irradiance G_{water} in W/m^2:

$$G_{water} = G^* \frac{I_{SC,Cell_3}}{I^*_{SC,Cell_3}} \qquad \textit{Eq. XVIII}$$

where

$G^* = 1000W/m^2$, the irradiance corresponding to standard conditions,

$I^*_{SC,Cell_3}$ is the cell short-circuit current in A at standard conditions of $1000W/m^2$

If the cell is located underneath a SODIS bottle, the value of the irradiance G_{water} will be lower than the solar irradiance G as the solar irradiance has to cross the bottle and the polluted water.

If the cell is located on top of the container within a solar water pasteurizer, assuming no extra irradiance coming from the reflector, the value of the irradiance G_{water} will be equal to the solar irradiance G. If there are reflections, the former value will be higher.

d) Water Cell temperature – Water temperature estimation - T_{Water_Cell}

From the water unit open-circuit voltage of cell 4, $V_{OC,Cell_4}$, we calculate the water cell temperature T_{Water_Cell} in ℃:

$$T_{Water\_Cell} = T^*_{Water\_Cell} + \frac{1}{\beta}\left[V_{OC,Cell_4} - V^*_{OC,Cell_4} + \frac{kT_{Water\_Cell}}{e} ln\left(\frac{G^*}{G}\right)\right] \qquad \textit{Eq. XIX}$$

where

$T^*_{Water\_Cell}$ is the cell temperature at standard conditions (25℃),

β is the V_{OC} temperature coefficient at the irradiance level G, given by the manufacturer,

$V^*_{OC,Cell_2}$is the open-circuit voltage of the cell at standard conditions (25℃), given by the manufacturer,

$\frac{kT^*_{Water\_Cell}}{e}$ is the thermal voltage, ($0.025mV\ at\ 25$℃),

$G^* = 1000W/m^2$, the irradiance corresponding to standard conditions, and

G is the solar irradiance, obtained by the cell 3 in the water unit.

From this water cell temperature we can then estimate the water temperature inside a SODIS bottle or a water pasteurizer container.

This clean water PV sensor can be integrated in all solar water technologies. In this project we are focusing on two of them: SODIS and solar water pasteurization. Now we are describing how to use the sensor in each of the technologies and how to obtain the main information parameters required for the clean/no clean water decision.

4.2.1 Clean Water PV Sensor for SODIS

The clean water PV sensor can be integrated in SODIS by placing the reference unit external to the bottle and avoiding possible shading from it, and by placing the water unit underneath the bottle, such as indicated in Fig. 20. With this configuration, we obtain the four main parameters indicated previously (solar irradiance, UV irradiance, irradiance through the bottle and water cell temperature), and from them, we can calculate and/or estimate the following additional information parameters: sunshine hours, absorbed irradiance in the bottle, transmittance changes and water temperature. With all this information, we can decide if the water is clean or not, as per established by the SODIS clean water criteria: 6 hours of sunshine if sunny, 2-3 days if cloudy; or equivalent UV dose received.

a) Sunshine hours

Sunshine hours can be estimated from the solar irradiance data, provided by the reference unit (solar cell 1), as we have studied in the chapter 3. From the reference unit (solar cell 1) we obtain the global solar irradiance, and from this value, we can estimate the sunshine duration using the Olivieri algorithm and considering the uncertainty associated to daily values.

b) Absorbed irradiance

The water unit cell (cell 3) will provide the solar irradiance that has reached the solar cell G_{Water}, the solar irradiance that has crossed the bottle and has not been absorbed. By calculating the difference with the total solar irradiance G measured by the external reference cell (cell 1) we can calculate the solar irradiance that has been absorbed in the

bottle. The water by its nature absorbs the FIR and the cell does not detect this change, so we obtain the absorbed irradiance in the bottle from the UV to the NIR:

$$G_{Absorbed} = G - G_{Water} \qquad \textit{Eq. XX}$$

c) Transmittance changes

We can also calculate transmittance changes in the water if we compare the irradiance through the water and the solar irradiance. These transmittance changes might allow us to detect changes in the water content as the pollutant disappears if the pollutant has an absorption response in the same part of the spectrum as the solar cell (UV, Vis & NIR). To detect transmittance changes, we need to convert the measured short-circuit currents both from cell 1 and cell 3 to standard conditions (1000 W/m^2), which means to obtain the short-circuit current of the cell at standard conditions (STC), the value that we obtain as a main parameter after calibration. If there are no transmittance changes, the output should be a constant, the value that we measured. When there are transmittance changes, the value of the short-circuit current at STC of the cell underneath the bottle (cell 1) will change, indicating changes within the bottle. The short-circuit current at STC of the reference cell (cell 3) should remain constant. This effect has been observed in recent works [42].

$$I^*_{SC,Cell_1} = G^* \frac{I_{SC,Cell_1}}{G} \qquad \textit{Eq. XXI}$$

$$I^*_{SC,Cell_3} = G^* \frac{I_{SC,Cell_3}}{G_{water}} \qquad \textit{Eq. XXII}$$

d) Water temperature

From the water cell temperature, we can estimate the water temperature inside the bottle if there is a good thermal contact between the front part of the encapsulated cell and the bottle, and it will improve if the material on the back of the encapsulation is thermally insulating. To estimate the water temperature, we can estimate the thermal losses in the interface between the bottle and the encapsulated cell and then include them in the system. A very simple initial approach would be to assume that the encapsulated cell is well insulated in all sides except in the front one, where the heat from the water reaches the cell only by conduction with a certain thermal resistance through the plastic bottle and the encapsulation:

$$T_{Water} = T_{Water\_Cell} + R_{bottle-encapsulation}(P_{Sun} - P_{Water}) \qquad Eq.\ XXIII$$

$$P_{Sun} = G \cdot A_{Cell4} \cdot \eta \qquad Eq.\ XXIV$$

$$P_{Water} = G_{Water} \cdot A_{Cell4} \cdot \eta \qquad Eq.\ XXV$$

$R_{bottle-encapsulation}$ is the thermal resistance between the plastic bottle, through the encapsulation, to the solar cell 1 ($℃/W$), $P_{Sun}$is the solar power on the cell 1 (W), $P_{Water}$is the electrical power on the cell 1 (W), A_{Cell4} is the cell area (m^2), η is the solar cell efficiency (%).

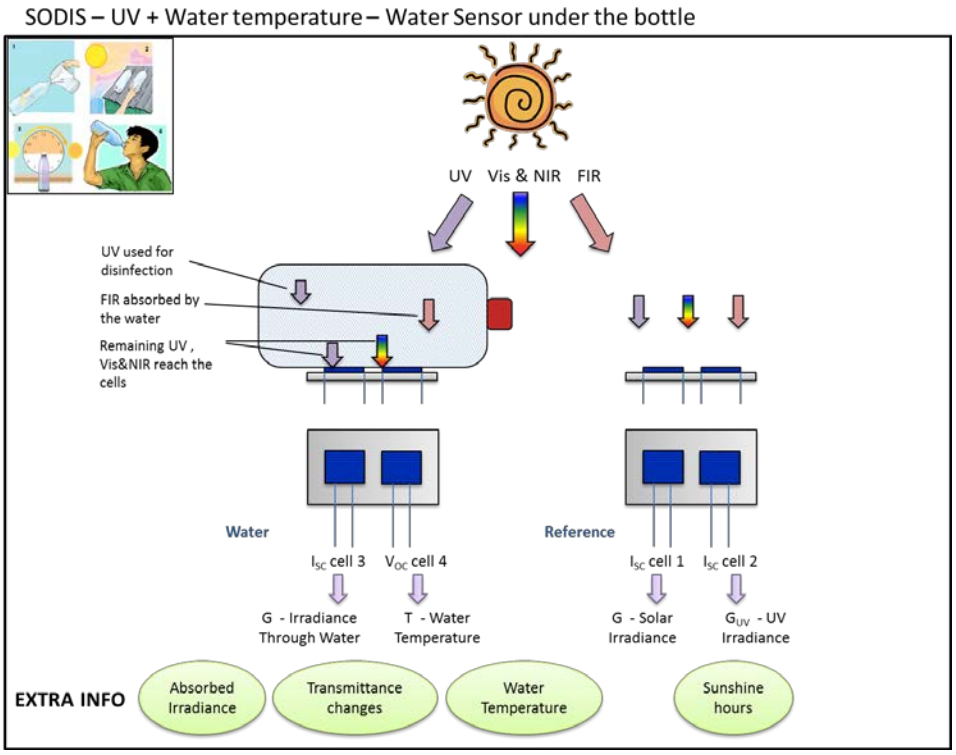

Fig. 20: Clean water PV sensor integrated in the SODIS technology, with the reference unit external to the bottle and the water unit underneath the bottle, obtaining information on global irradiance, UV irradiance, sunshine hours, absorbed irradiance in the bottle, transmittance changes and water temperature.

4.2.2 Clean Water PV sensor for Solar Water Pasteurization

For the case of the solar water pasteurizer, the clean water PV sensor can be integrated by placing the reference unit external to the entire system (avoiding possible shading from it as in the SODIS bottles) and by placing the water unit on top of the water

container within the system, as shown in Fig. 21. We obtain the four main parameters of the sensor (solar irradiance, UV irradiance, irradiance on the container and water cell temperature), and from them, we can calculate and/or estimate the following information parameters: sunshine hours, irradiance on the container and water temperature. The main parameter is the water temperature, and the water will be clean or not depending on if the water has reached pasteurization temperature for a sufficient time as to degrade the pollutant in the container. For example, some microorganisms such as E. coli, rotavirus, Vibrio cholera, Salmonella thyphi and Shigella sp, require a temperature of 60ºC during 1 minute to get 90% of them destroyed [6].

a) Sunshine hours

Sunshine hours is calculated following the same procedure described in the SODIS section, although in this case we need to be careful as the use of a solar cell as irradiance sensor is not as accurate as in SODIS because solar pasteurization uses all the solar spectrum to convert it to thermal energy and the solar cell only part of it. However, considering the low-cost approach followed and that most of the solar energy is in the UV-Vis-NIR range, it will provide sufficient information to know how the solar irradiance conditions are despite the spectral mismatch.

b) Irradiance on Container

Cell 3 gives the irradiance on the container, which will be equal to the total solar irradiance measured by Cell 1 if there is no reflector, and higher if there is an effective reflector. Same considerations as for sunshine hours calculation applies in this case as there is no spectral match between the applications.

c) Water temperature

Water temperature is the most useful parameter in water pasteurization. In this case, good thermal contact must be obtained between the back sheet of the cell encapsulation and the water container. The front material of the encapsulated cell should be as thermal insulating as possible to avoid thermal losses. In this case, to estimate the water temperature, we consider a thermal resistance between the encapsulation and the container, and we calculate the power directly from the irradiance measured in the container:

$$T_{Water} = T_{Water\_Cell} + R_{encapsulation-container}(P_{Sun} - P_{Water}) \qquad Eq.\ XXVI$$

$$P_{Sun} = G_{Container} \cdot A_{Cell4} \cdot \eta \qquad \textit{Eq. XXVII}$$

$$P_{Water} = G_{Container} \cdot A_{Cell4} \cdot \eta \qquad \textit{Eq. XXVIII}$$

$R_{encapsulation-container}$ is the thermal resistance between the plastic container, through the encapsulation, to the solar cell 1 ($℃/W$), $P_{Sun}$is the solar power on the cell (W), $P_{Water}$is the electrical power on the cell 1 (W), A_{Cell4} is the cell area (m^2), η is the solar cell efficiency (%).

In this case, we will consider the use of thermocouples for liquid-immersion if the current cost is affordable and it is feasible to insert the thermocouple in the liquid without affecting the water treatment process (we need to consider that for developing regions inserting something in the water might actually introduce more contaminants in the water that can affect the final performance of the system).

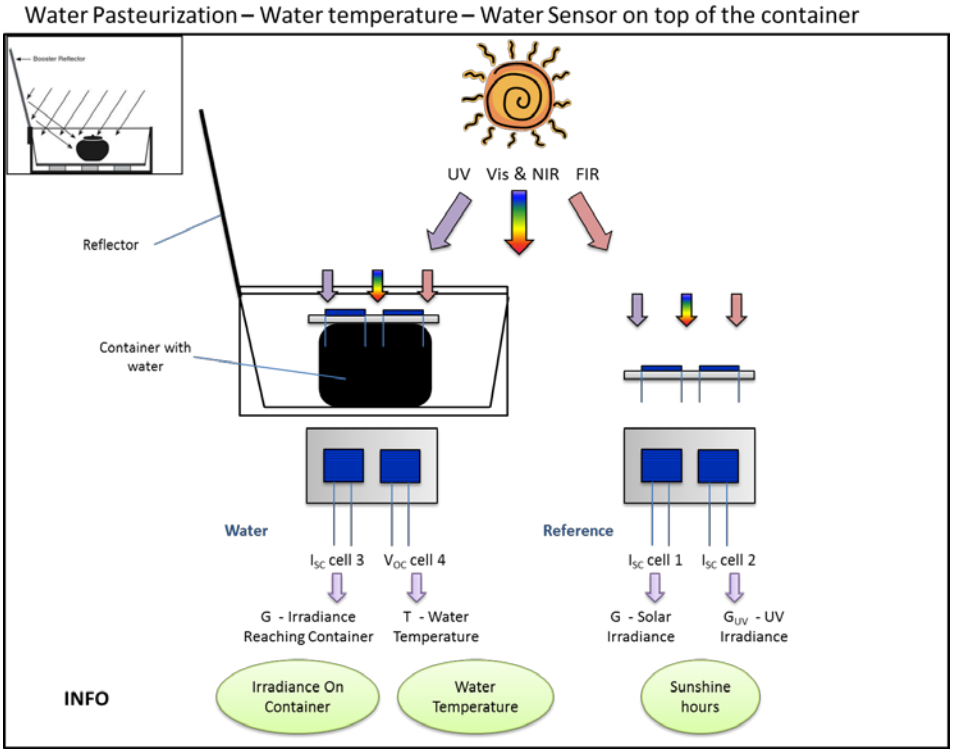

Fig. 21: Clean water PV sensor integrated in the solar water pasteurization technology, with the reference unit external to the bottle and the water unit on top of the water container, obtaining information on global irradiance, UV irradiance, sunshine hours, irradiance on the container and water temperature.

4.3 Manufacturing

A first sensor that can be used in SODIS but adapted to solar water pasteurization has been manufactured. Detailed design aspects such as size and materials are described below, followed by the final manufacturing process.

4.3.1 Size

SODIS uses transparent PET bottles and solar water pasteurization uses containers that can be bottles or in other shapes painted in black to optimise the absorption of solar energy in the container. For this generic sensor, we are going to focus on the PET bottles from SODIS, as they can be also used as containers for solar water pasteurization units by simply painting them in black, and for their extended use in developing countries. In general, the most common sizes for PET bottles used in SODIS are small bottles of 1-2 L [43]. The main issue for the sensor based on solar cells is that the bottle is round and the conventional cells that we are going to use in this first sensor are flat, so for the water unit of the sensor (the one placed underneath the bottle) we need to minimise the optical losses between the flat cells and the round bottle. We used thin, elongate solar cells for this purpose, calculating from the bottle dimensions the most appropriate dimensions for the sensor solar cells.

Different bottles of different sizes, ranging from 1.5L to 2L were analysed, studying their perimeters and therefore their diameters, as well as the elongate flat parts on which locate the sensor (Fig. 22). Perimeters were from 270mm to 317mm, and the elongate flat parts, which are the parts in which the bottle is flat and without drawings that can produce optical losses, were from as small as 75mm to the size of the full bottle, 200mm.

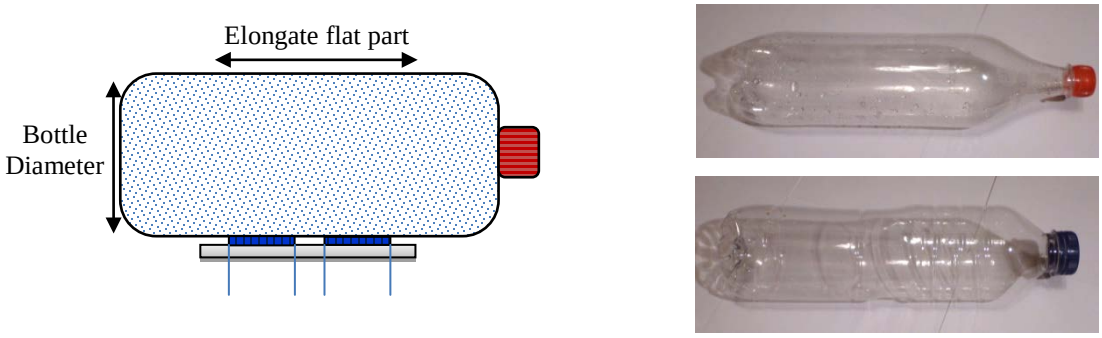

(a) (b)

Fig. 22: a) Schematics of a PET bottle with the water unit of the sensor below showing the two main dimensions to consider: bottle diameter and elongate flat part; and b) example of PET bottles: on the top a bottle completely flat and on the bottom a bottle with non-flat parts not suitable for placing the sensor underneath.

If we consider a cross-sectional view of the PET bottle, Fig. 23, we can see the bottle with its radius, r_{bottle}, and the cell underneath with its width w_{cell}. We define D_{cell} as the distance from the centre of the circumference to one edge of the cell, $w_{cell}/2$, and θ as the angle between the radius that crosses the centre of the cell and D_{cell}. h_{gap} is the distance between the edge of the cell and the bottle, where the optical losses are maximum. From the geometry, equations XXIX and XXX give the values of D_{cell} and h_{gap}. In order to minimise the optical losses produced in the gap between the bottle and the cell, we need to minimise the angle θ so D_{cell} is approximately equal to r_{bottle}, but maximising w_{cell} so we have sufficient cell area to capture the incoming sunlight. We need to establish a trade-off between the optical losses due to the different geometries and the need for sufficient solar cell area.

$$D_{cell} = \frac{w_{cell}/2}{sen\left(arc\ tg\left({}^{w_{cell}/2}/_{r_{bottle}}\right)\right)} \qquad Eq.\ XXIX$$

$$h_{gap} = R\left(1 - cos\left(arc\ sen\left({}^{w_{cell}/2}/_{r_{bottle}}\right)\right)\right) \qquad Eq.\ XXX$$

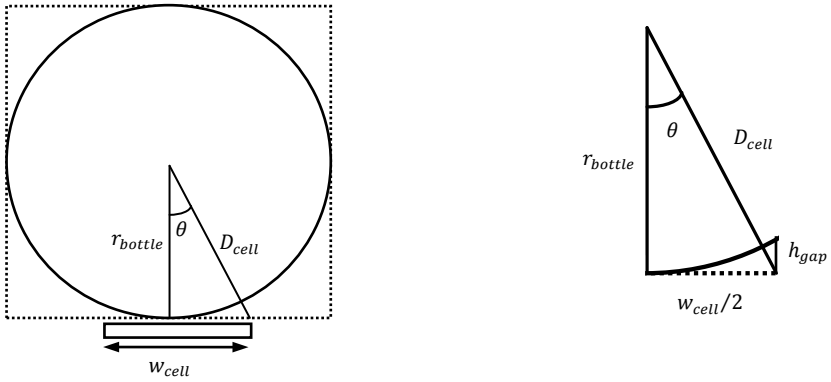

Fig. 23: Cross-sectional view of the bottle with the cell underneath, showing the radius of the bottle, r_{bottle} , and the width of the cell, w_{cell}. To minimise the optical losses due to the geometry, D_{cell} must be approximately equal to r_{bottle}, with a trade-off between losses and cell area.

For example, for the smallest bottle, of 270mm perimeter, we have a radius of 43mm. With a cell width of 4mm we would obtain a D_{cell} of 43.05mm and a h_{gap} of about 0.05mm, and with a cell width of 6mm a D_{cell} of 43.1mm and a h_{gap} of about 0.1mm, which are acceptable values for cell area and losses in this application. So a cell between 4mm-6mm width would be suitable.

Regarding the length of the cell, if we consider the minimum elongate flat part of the three bottles, it comes down to 75mm, so in order to place two cells with a minimum separation of 2mm between them, the length of the cell could be up to 36mm.

4.3.2 Materials

Materials selection can be divided into the solar cell and the rest of the encapsulation into a complete module, plus the low cost UV filters.

Regarding the solar cells, there are different technologies available in the market, including monocrystalline silicon solar cells, multicrystalline silicon solar cells, thin films solar cells using amorfous silicon, cadmium-telluride, crystalline silicon, etc. For this project we have used monocrystalline silicon solar cells from the Institute of Solar Energy (IES-UPM) in Madrid, Spain. The cells are LGBC solar cells originally manufactured by BP Solar, with an initial size of 6mm x 116mm, including two bus bars of 3mm each, one

at each side of the cell (Fig. 24a). Average efficiency of the cells is 16.8% at STC and the V_{OC} temperature coefficient is -2.3mV/ºC. The cells were cut to a length of 30mm, so the final solar cell size for the sensor was 6mm x 30mm (Fig. 24b).

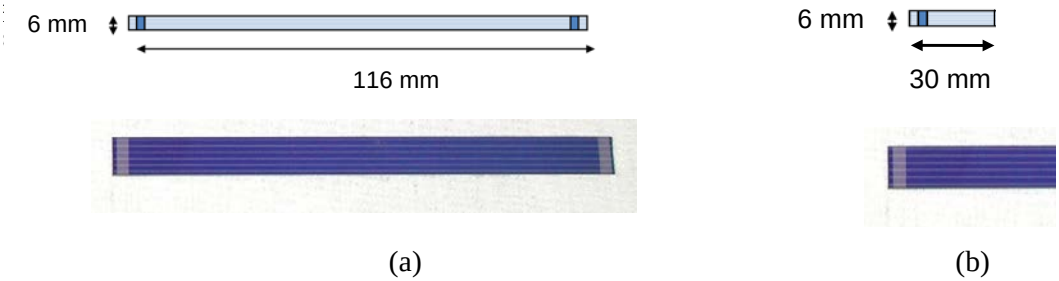

(a) (b)

Fig. 24: a) Original monocrystalline silicon solar cell from IES-UPM (6mm x 116mm), b) Cells for the clean water PV sensor after cutting to a size of 6mm x 30mm.

Encapsulation materials should be selected according to the final solar water treatment system and the location of the sensors to achieve good thermal contact with the system as we already discussed earlier in the chapter. But for this initial sensor we used a standard encapsulation based on a 1mm glass cover consisting of a microscope slide of clear glass, a clear silicone (Wacker Silgel 612) and a black back cover of Tedlar®, which are standard materials in PV modules. We use black Tedlar® to avoid unwanted reflections on the cells serving as sensors.

For the low-cost UV filter, we explored the possibility of using a conventional UV filter from photography, consisting of a 62mm diameter and 1.78mm thickness UV filter from Hama®; and an architectural window film for glass protection and safety provided by the Portuguese company Impersol Lda, the SCL SR PS4 Llumar 0.1mm thickness film [44, 45] (Fig. 25a and Fig. 25b). Transmittance of both filters were analysed by using a UV-Vis spectrophotometer. The glass filter was measured directly in the spectrophotometer, but the UV film was previously attached to a 1mm thickness microscope clear slide, in order to measure the final transmittance in this configuration that it is going to be used in the final sensor. A quartz slide of 1mm was also used as a reference. From the film manufacturer data we know that a 3.75mm thickness clear window glass without film has 83% total solar transmittance, 90% visible light transmittance and 29% UV rejection. With the SCL SR PS4 film on top, the window achieves 81% total solar transmittance, 89% visible light transmittance, 95% UV rejection. The glass UV filter manufacturer does not provide any

information about spectral transmittance. Fig. 26 shows the transmittance of both the glass filter and the film on 1mm quartz. We can observe that the Hama glass filter transmittance in the UV is higher than the film. It cuts at a lower wavelength of 329nm, allowing UV light to pass through, with a final overall UV blockage of 59%. The UV film on clear slide rejects 90% of the total UV with a cut-off wavelength of 383nm, vs. the 95% UV rejection given by the manufacturer. It reaches 88% visible light transmittance vs. the 90% visible transmittance provided by the manufacturer. These differences are mainly due to the different type of glass used as a support for the film. As a reference, the quartz slide only blocks 8% of the total UV. Finally, we selected the architectural film as a low-cost UV filter for our application.

(a)

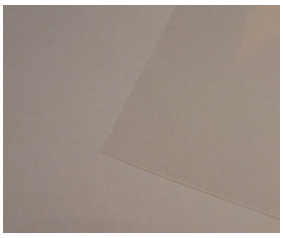

(b)

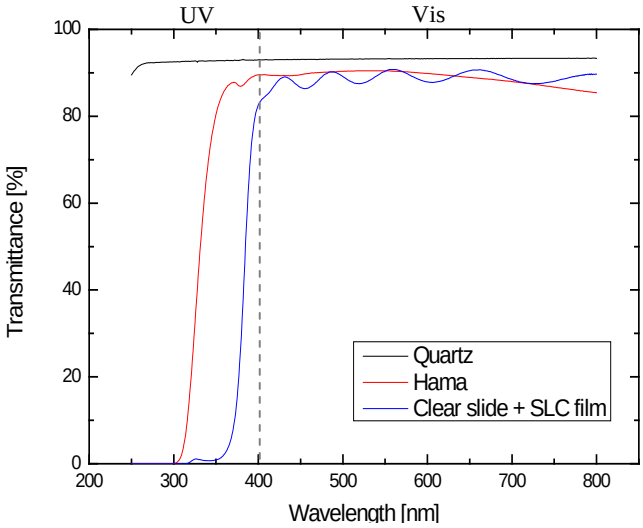

(c)

Fig. 25: Low cost UV filters: a) photographic UV filter from Hama; b) SCL SR PS4 Llumar UV film from Impersol; and c) transmittance of the two UV filters tested, with the film filter with a higher rejection of the UV content.

We also need to consider that we do not aim to measure the total UV irradiance accurately but the UV irradiance that is available to the water purification process, i.e. the UV irradiance that reaches the water within the bottle, including the transmission losses when the light crosses the PET bottle. Fig. 26 shows the transmittances of the PET bottle, cutting at 325nm and therefore using only the UVA light (320nm-400nm); and the clear slide plus the UV film, cutting at 383nm.

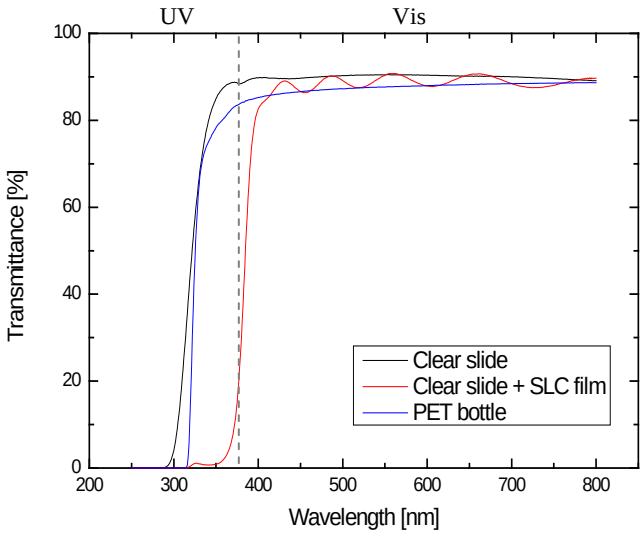

Fig. 26: Transmittance of the clear slide used to encapsulate the solar cell, the PET bottle and the UV blocking film on clear slide.

4.3.3 Manufacturing process

Fig. 27 presents the final design for each of the units of the sensor, showing the solar cells connected to the tabs and the black Tedlar backsheet. Fig. 27a shows a top view and Fig.27b a side view, showing the encapsulant and the clear glass. It also shows the UV filter location in one of the cells for the case of the reference unit.

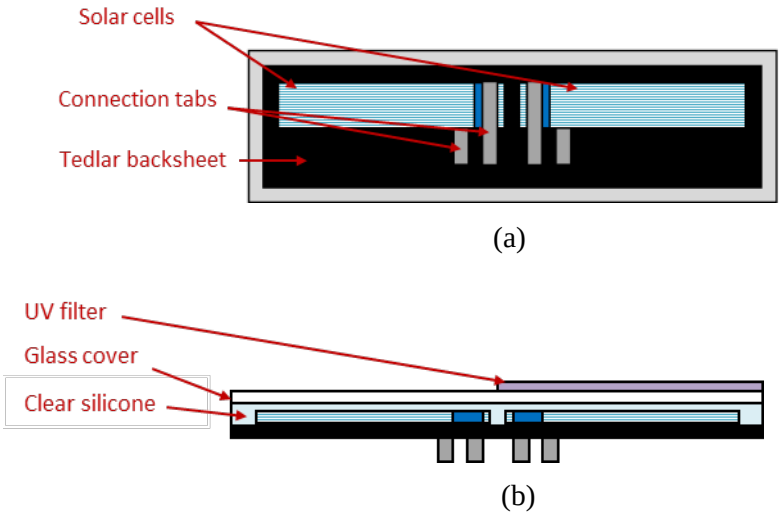

Fig. 27: Design of the units of the sensor, showing the two solar cells with the bus bars soldered to the tabs, the black Tedlar backsheet, the encapsulant, the glass cover and the UV filter: a) Top view of the designed unit, b) Side view.

The manufacturing process starts with the cut of the original solar cells of 6mm x 116mm to the required size of 6mm x 30mm (Fig. 28a). So we cut the cell only in length. The cell cut was conducted at the facilities of CENTESIL (Centro de Tecnología de Silicio Solar) in Madrid, using an automatic dicing saw. After cutting, cells were measured in an indoor solar simulator (AM1.5G) at STC at IES-UPM labs, obtaining the I_{SC} in order to match the cells for the sensor units, using cells of similar short-circuit current for each unit (results can be found in the Annex).

Next step is to wire the cells to the connection tabs (Fig. 28b), which was done by soldering in the hot plate using solder paste (Sn-Ag). Once the cells were soldered, we prepared the Tedlar® and place the cells on top for encapsulation. Encapsulation used a clear silicone of two components, Wacker Silgel 612, in a ratio of 1.5:1. It was mixed and then vacuumed to remove possible air bubbles and then poured into the Tedlar and cells, covering with the glass cover (Fig. 28c). Curing was at room temperature (24h at 25ºC).

After the encapsulation (Fig. 28d), wires were soldered to the tabs and then connected to screw terminals, where the external wires of 0.5m each were connected (Fig. 28e). Then the units were fixed into small boxes that protect the wiring and have sufficient room for including the electronics of the sensor in the future. Silica was added to avoid moisture. Shunt resistors of 0.1Ω-1% were connected to the cells that will be measuring I_{SC}. Fig. 28f shows the final sensor unit and Fig. 28g the two units that the sensor is comprised of. The UV filter film was not included at this point as it was required that the cells were calibrated first so they have the same reference. Fig. 28h shows an example of the sensor including an UV filter.

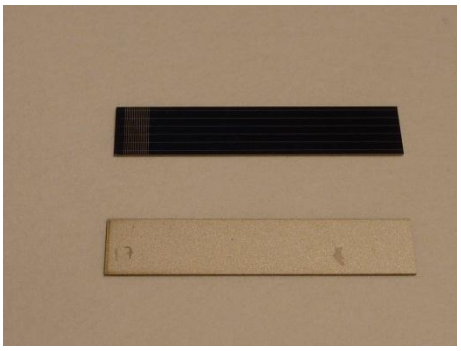

(a)

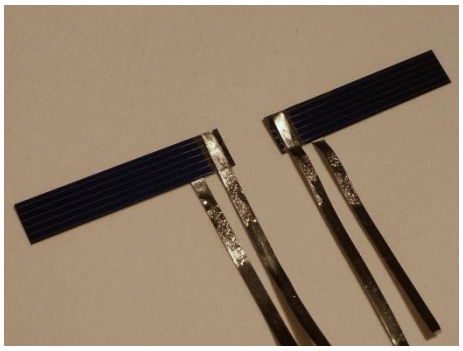

(b)

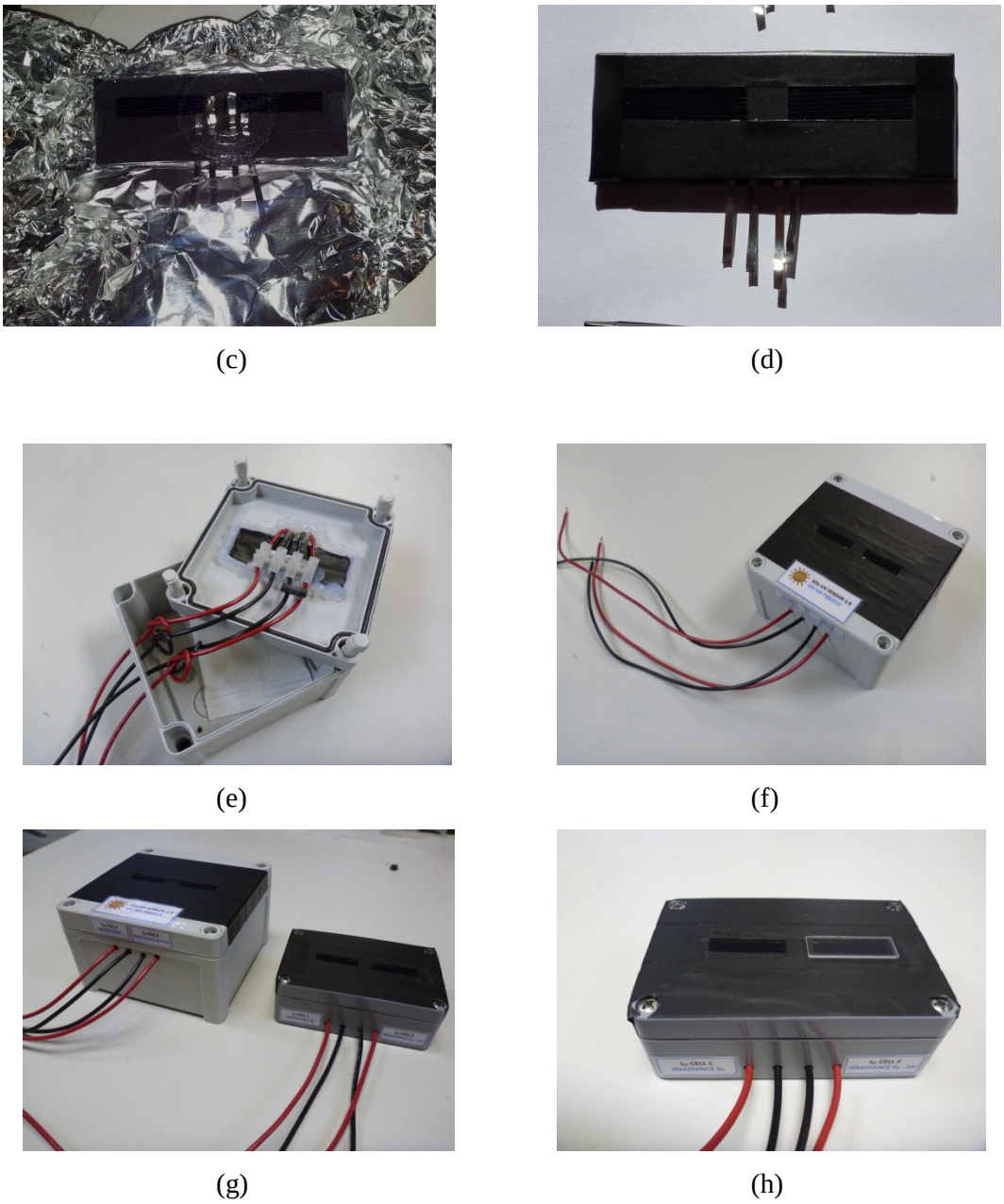

(c) (d)

(e) (f)

(g) (h)

Fig. 28: Cells after each step of the manufacturing process of the sensor units: a) solar cells cut to 6mm x 30mm, b) cells soldered to the tabs, c) cells under encapsulation with clear silicone and glass cover, d) encapsulated units, e) cells fixed to the box with shunt resistor and external wires connected, f) final sensor unit, g) final sensor comprising the two units, h) example of the sensor unit including an UV filter.

4.4 Initial Calibration

The clean water PV sensor must be initially calibrated. The calibration consists of an initial exposure to sunlight to reduce initial photon degradation effects and to stabilise the cells, an indoor characterisation and an outdoor calibration. The initial exposure was

conducted at University of Jaén (Jaén, Spain), the indoor characterisation at the lab facilities of IES-UPM (Madrid, Spain) and the outdoor calibration at University of Jaén.

4.4.1 Initial exposure to sunlight

It consists in exposing the solar cell for a total of 5kWh/m^2 open-circuited to reduce initial photon degradations effects. It is specified by the IEC 61215 international standard for 'IEC 61215 – Crystalline silicon terrestrial photovoltaic (PV) modules. Design qualification and approval' [18]. This procedure was conducted at the University of Jaén outdoor facilities, during two winter days, 29th January 2013 and 1st February 2013, accumulating a received irradiance of 5.09kWh/m^2. Fig 29 shows the global solar irradiance on the horizontal plane for the two days of exposure.

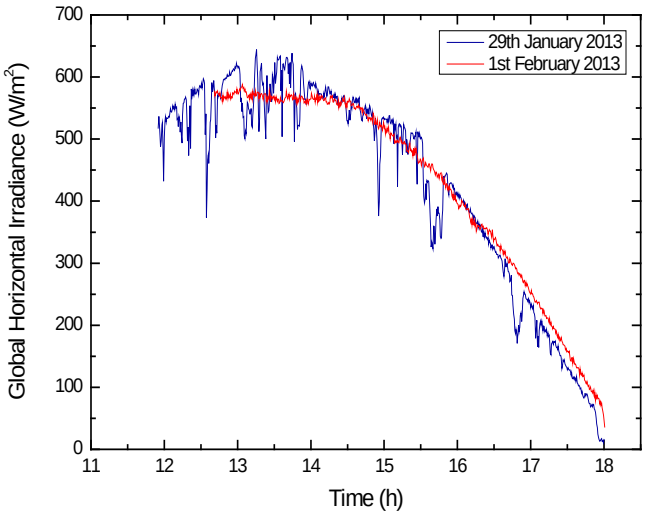

Fig. 29: Global solar irradiance on the horizontal plane for the two days of initial exposure, 29th January 2013 and 1st February 2013, accumulating a total of 5.09kWh/m^2.

4.4.2 Indoor calibration

It was conducted at the IES-UPM labs, using an indoor solar simulator and the AM1.5G spectrum at the STC conditions, 1000W/m^2 and 25ºC (Fig. 30). We measured the I_{SC} of cells 1, 2 and 3 and the V_{OC} of cell 4 at 1 sun and 25ºC, obtaining the main reference parameters of the sensor:

$$I^*_{SC,Cell_1} = 53.26mA$$
$$I^*_{SC,Cell_2} = 54.30mA$$
$$I^*_{SC,Cell_3} = 55.18mA$$
$$V^*_{OC,Cell_4} = 595mV$$

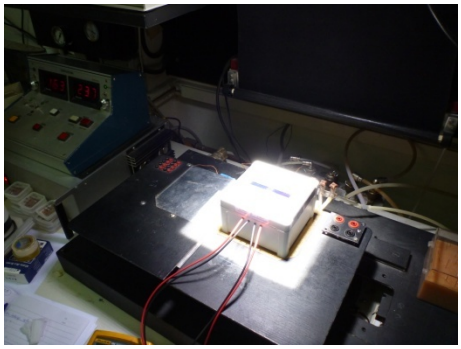

(a)

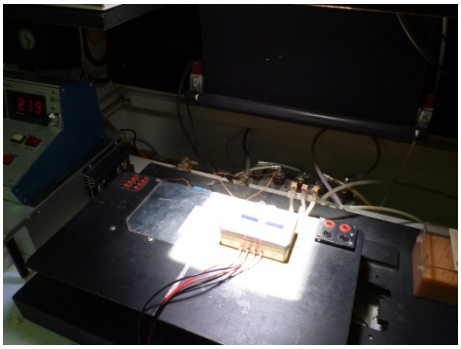

(b)

Fig. 30: Sensor units under calibration at the indoor solar simulator at IES-UPM labs, measuring $I_{SC,Cell\_1}$, $I_{SC,Cell\_2}$, $I_{SC,Cell\_3}$ and $V_{OC,Cell\_4}$ at STC (1000W/m^2, 25ºC).

4.4.3 Outdoor calibration

To minimise uncertainties of the indoor calibration due to the artificial lamp and temperature conditions of the lab, outdoor calibration was conducted at the University of Jaén facilities, placing the solar cells on a tracker and following the specifications of the international standard 'IEC-60904-2 - Photovoltaic devices. Part 2: Requirements for reference solar cells' [36]. With the cells on tracker (Fig. 31), we measured the I_{SC} of cells 1, 2 and 3, the V_{OC} of cell 4 and the T of cell 4 under natural sunlight for a period of two hours. The global irradiance on the normal plane was measured by a pyranometer placed on the tracker. Fig. 32 shows an example of the linear fitting between the I_{SC} of one of the solar cells and the global irradiance on the plane, obtaining the calibration value. For the V_{OC} of cell 4, we waited for the cell temperature to stabilise prior to the data taking. We obtained the main reference parameters of the sensor:

$$I^*_{SC,Cell_1} = 54.78mA \text{ @ } 1000\ W/m^2$$
$$I^*_{SC,Cell_2} = 55.22mA @ 1000W/m^2$$
$$I^*_{SC,Cell_3} = 56.23mA @ 1000W/m^2$$
$$V^*_{OC,Cell_4} = 505.016mV @ 1035W/m^2 \ and \ \ T_{Cell_4} = 64.16\ ℃$$

Converting into standard testing conditions, 1000W/m^2 and 25ºC, we obtained the following reference values:

$$I^*_{SC,Cell_1} = 54.78mA$$
$$I^*_{SC,Cell_2} = 55.22mA$$
$$I^*_{SC,Cell_3} = 56.23mA$$
$$V^*_{OC,Cell_4} = 594.12mV$$

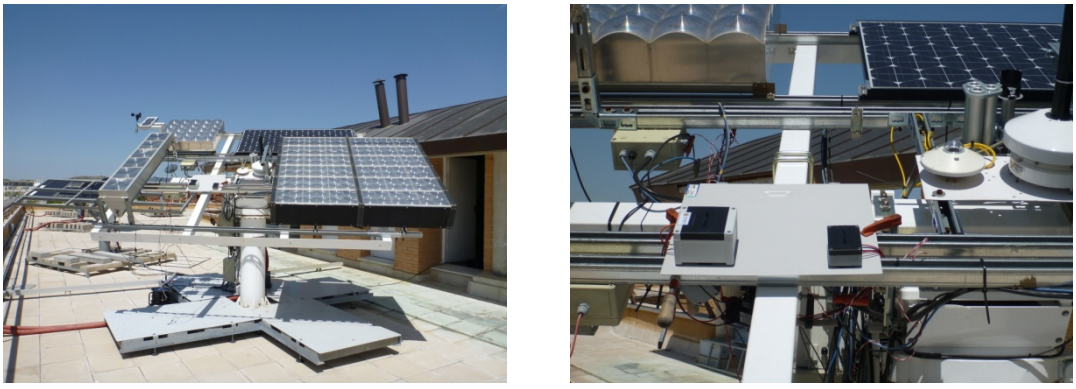

(a) (b)

Fig. 31: Sensor units under calibration on the tracker at the outdoor solar facilities at University of Jaén, measuring $I_{SC,Cell\_1}$, $I_{SC,Cell\_2}$, $I_{SC,Cell\_3}$, $V_{OC,Cell\_4}$ and T_{Cell_4} under natural sunlight (irradiance measured by the pyranometer in the tracker).

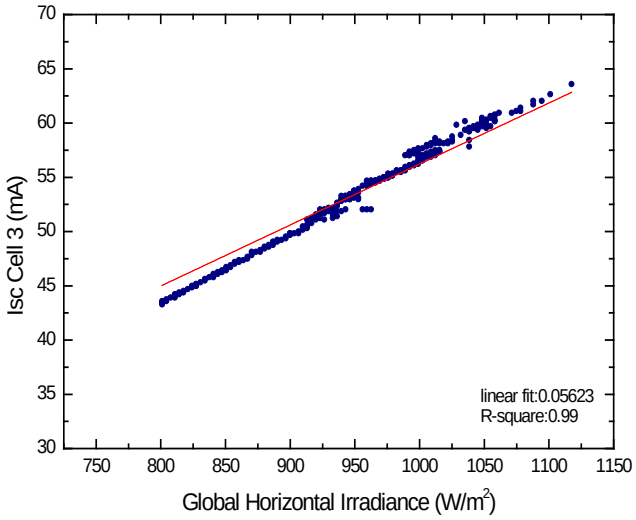

Fig. 32: Example of one of the cells short-circuit current outdoor calibration against a calibrated global pyranometer mounted on the same plane as the cell.

5. TESTING OF THE NEW CLEAN WATER PV SENSOR

Once the cells in the sensor were calibrated, the performance of the clean water sensor was tested. Four types of tests were conducted, including an initial test with all the cells measuring over the span of a day, a specific calibration of the new UV sensor, a test with tap water and a preliminary experiment with polluted water.

The objective of these tests is **to determine if the new sensor provides useful data to help the water quality monitoring**. More specifically, we aim to study the following parameters measured by the solar cells: sunshine duration, total global irradiance and irradiance at the bottom of the bottle, UV irradiance and water temperature. We will compare these parameters with the water microbiological analysis and the reference values of UV and temperature given in the literature for the SODIS process, and determine whether the new sensor is useful or not for the water purification and if so, under which conditions and limitations.

5.1 Characterisation as sunshine duration sensor

To verify the performance of the SolWat sensor as sunshine duration recorder, the sensor was subjected to different days of exposure under natural sunlight and its output compared with a reference global horizontal pyranometer. The set-up is shown in Fig. 33, where the sensor is placed horizontally and in the same plane of the global pyranometer. Fig. 34 shows the performance of the SolWat sensor cells when used to measure global horizontal irradiance in comparison with the reference data from the pyranometer. Two different climatic conditions are shown, corresponding to sunny and cloudy weather, and good agreement is shown between the global measured by the PV cells and the reference global irradiance given by the pyranometer.

From the global horizontal irradiance measured by Cell 1, we calculated the sunshine duration and then compared it with the sunshine duration calculated by the pyrheliometer from the weather station and the one calculated by the pyranometer. For both the pyranometer and the cell, the selected method was the Olivieri one, as we demonstrated in Chapter 3 that was the most suitable one for the PV cell. In Table IV we

can observe the results for different days of testing, with the cell and the pyranometer performing similarly and in all the cases underestimating the sunshine duration value. It is important to remember that all the SD pyranometric algorithms have been developed for temperate climates and that we also observed that this algorithm underestimates in the summer months (see Chapter 3). This is not a critical issue as for water treatment applications it is always a good practise to be conservative. In summary, the SolWat sensor can be used to measure both global horizontal irradiance and sunshine duration.

(a) (b)

Fig. 33: SolWat sensor units under sunlight measuring global horizontal irradiance and sunshine duration (13th April 2013).

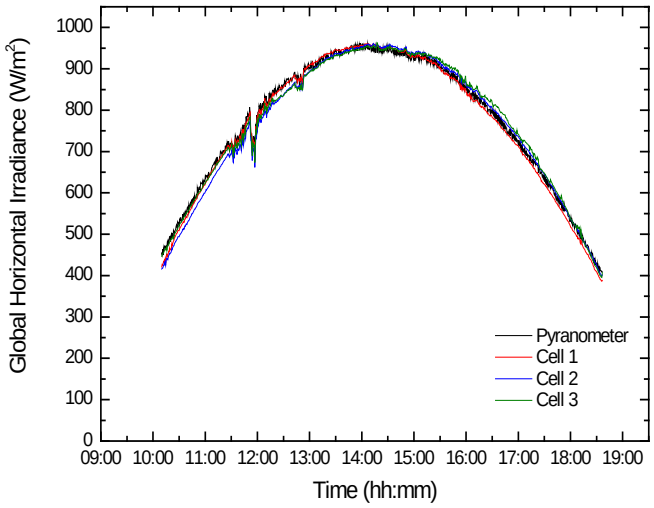

(a)

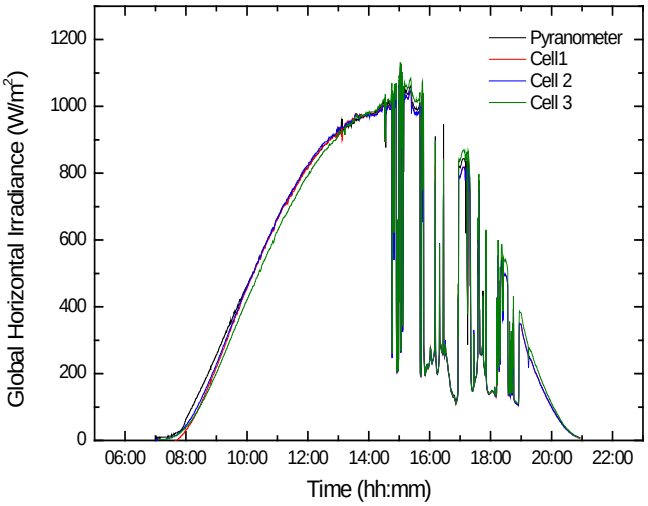

(b)

Fig. 34: Global horizontal irradiance measured by the pyranometer and global horizontal irradiance measured by the SolWat sensor cells for two different days: a) 13th April 2013, sunny weather; and b) 24th April 2013, with partially cloudy weather.

Table IV: Daily totals of SD for several days using the pyrheliometric method and the Olivieri algorithm for the pyranometer and the cell and differences with pyrheliometric SD.

Date	SD – Pyrhel (h)	SD – Olivieri Pyran (h)	SD – Olivieri Cell 1 (h)	Difference Pyran (h)	Difference Cell 1 (h)
13/04/2013 (partial)	8.45	6.57	6.57	-1.88	-1.88
14/04/2013 (partial)	8.47	6.55	6.55	-1.92	-1.92
23/04/2013 (partial)	9.65	6.12	6.12	-3.53	-3.53
24/04/2013 (complete)	9.7	8.85	8.68	-0.85	-1.02

5.2 Characterisation as UV sensor

The UV irradiance is measured by the SolWat sensor using the UV film attached on the front surface of the solar cell 2. First, the UV film was attached to a microscope glass slide as per the manufacturer instructions, which suggested using the film on the inner side of the glass, i.e, the glass facing downwards leaving the film between the solar cell and the glass. The main reason was to protect the film from scratching if placed on the front surface directly. Once the film was attached to the microscope glass slide, we placed it

onto the encapsulated solar cell. To adapt optical refraction indexes and minimize optical losses, clear standard Vaseline (n=1.5) was used between the glass of the cell and the film and fixed with outdoor adhesive tape. This configuration was intended to be flexible and allowed changes of films or glasses, testing other materials. For a final design, clear encapsulating silicone would be used to fix the film permanently. However, several tests conducted in different days showed that this testing configuration was not suitable for this particular case. The two solar cells of this unit, solar cell 1 measuring irradiance and solar cell 2 measuring irradiance minus the UV, have a relatively small area (6mm x 30mm) and they are encapsulated one next to the other with a minimum distance of a few millimetres between them. Once the glass with the UV film was placed on top of the solar cell 2, this higher glass was sufficient to modify the sunlight reached by the solar cells due to edge effects, especially at small angles of incidence. This small difference was particularly critical as we were measuring the two solar cells differential output, so the error was too large and therefore this configuration not suitable for this particular case of small-area cells and close encapsulation.

Finally, a second solution was adopted, consisting of attaching the UV film directly onto the solar cell in order to avoid the previous problems. The film is very thin, 0.1mm vs 1mm of the microscope glass slide, so the edge effects should be minimized. A first test was conducted, measuring the UV output from the SolWat sensor and the UV output of a reference global UV sensor (Fig. 35a). This first experiment also presented a problem with the film attachment and a bubble appeared (Fig. 35b), affecting the SolWat UV output. This was due to a handling material error during attachment and should be easily corrected in future tests. Despite this error, we can observe a good correlation between the two UV signals, so there is a real potential for this type of sensor.

On the other hand, the reference global UV sensor measures total UV, including UVA and UVB, and the SolWat sensor measures only the UVA part of the UV spectrum, according to the cut-off wavelength of the filter (see section 4.3.2, materials). Another reason for differences between the sensors is due to the use of different glasses, clear glass in the UV reference sensor and standard glass in the microscope slide, which have different overall transmittances; and the supporting material of the UV film, which is PET and not glass. One could think that this is not a good solution for a low-cost UV sensor, but we need to consider the system requiring the sensor, in this case SODIS bottles. They use the

same material as the sensor, PET, and therefore the UV recorded by the SolWat sensor will be actually the same as the UV that the SODIS bottles are receiving. This UV will be more useful and accurate to detect clean water. The SolWat solution adopts the same principle as solar cells used as global irradiance sensors in power plants of the same technology, predicting more accurately the real performance of the PV plants (see section 4.1).

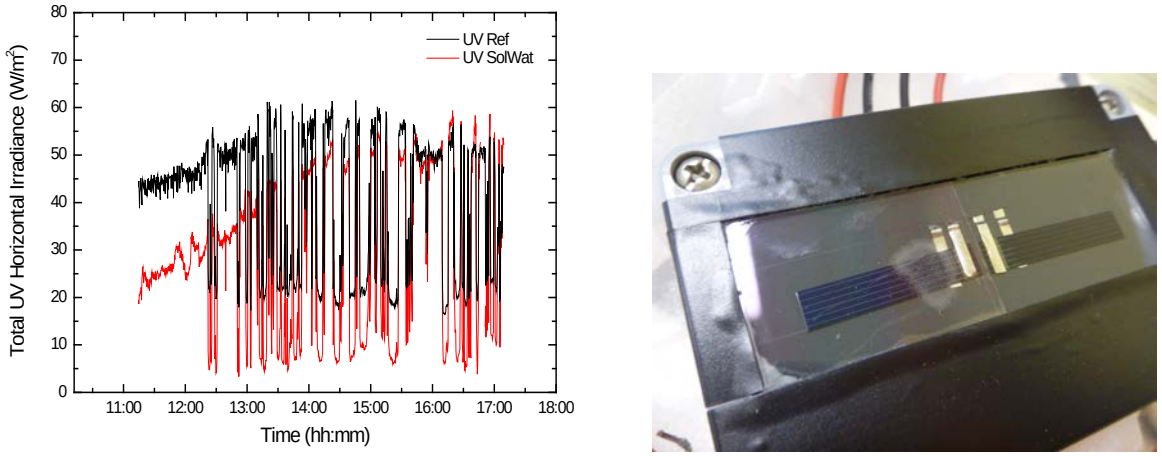

(a) (b)

Fig. 35: a) UV irradiance measured by the SolWat sensor and the global UV sensor used as a reference, showing the correlation between the two dataset (21st May 2013). Correlation is not as good as it should be due to a bubble originated in the UV film at the beginning of the experiment, as shown in b), but it indicates the potential of the low-cost UV sensor based in PV cells and UV-blocking architectural window films.

5.3 Experiments with tap water

By placing a solar cell under the bottle we can estimate the sunlight that is reaching the bottom of the bottle through the water depth. We can obtain data on how the turbidity affects the light transmission and then have another parameter to study when inactivating microorganisms in the water. A second cell aims to provide information on temperature, ideally, water temperature. This third group of tests consists of using a bottle filled with tap water and the two cells of the SolWat sensor underneath, and exposing the bottle to the sunlight along the day. Another option to measure the water temperature is to place a low-cost temperature sensor (LM35, 2.5€) in the bottle lid and insulate it electrically with silicone so it can work immersed in the water. Fig. 36 shows the set-up of the experiment, where a bottle of 1.5L (86mm water depth) has been placed horizontally and north-south orientated, with the SolWat sensor below; and with the special lid with the temperature

sensor inserted and a small tap for future experiments to take samples. Global irradiance and UV irradiance where also monitored.

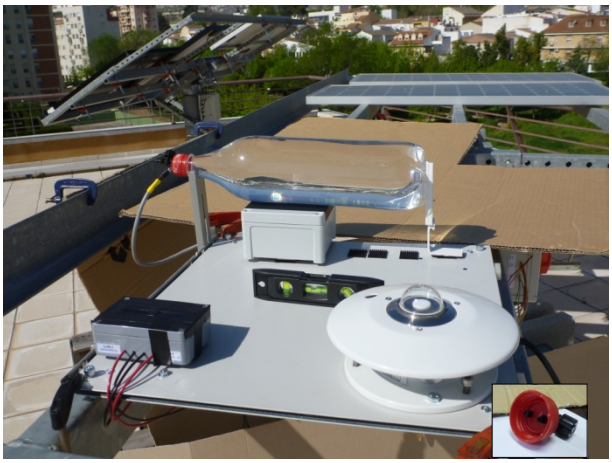

Fig. 36: Set-up of experiment with bottle filled with tap water and the SolWat sensor underneath to measure irradiance in the bottom of the bottle and water temperature (17th April 2013).

Fig. 37a shows the weather conditions during the experiment, with the global horizontal irradiance and the total UV irradiance. Fig. 37b gives the irradiance that reaches the bottom of the bottle. We can observe that during the central hours of the day that there is a concentration effect on the bottom of the bottle, due to the circular shape of the bottle and the clear water that act as a lens. This concentration effect is up to 3.7X and 3.85X at the peaks (Fig. 38a), and 2.65X average during the concentration effect that takes approximately 3h. Outside the central hours, the irradiance at the bottom of the bottle is dramatically reduced, reaching values of 88% absorption in the water. During the concentration period, the cell temperature also increases, to a maximum of 75ºC, following the concentration profile (Fig. 38b).The water temperature gets to a maximum of about 35ºC and then stabilises. The cell from the SolWat sensor has a small mass in comparison with the water volume in the bottle so the temperature measured by the cell is not representative of the entire water volume, but it also indicates when the concentration effect finishes.

During the span of the day, the cumulative global irradiance is 23.2MJ/m^2 (6453Wh/m^2) and the cumulative irradiance at the bottom of the bottle is 22.9MJ/m^2 (6372Wh/m^2), practically the same due to the concentration factor. Without this concentration, the irradiance at the bottom of the bottle should have been of approximately 2.8MJ/m^2 as most of the sunlight should have been absorbed in the water. This might mean

that the circular shape of the bottle is actually transmitting most of the light during the concentration effect and not absorbing it, which can have two different effects in the water purification process when the water is clear in comparison with a flat bag of water of the same depth. First, we could think that this effect would accelerate the process, as it seems that we get more light to the bottom of the bottle. But this means that the sunlight is not being absorbed through the bottle, so the first layers of water might not being affected by the UV disinfection, so it might be the opposite effect, and it decreases the rate of inactivation. On the other hand, the concentration is accumulating solar irradiance in a smaller area, which will heat up faster. This heat can be transferred by conduction to the rest of the bottle and contribute to increase the water temperature, improving the water disinfection.

The concentration effect is due to the low turbidity of the water and it is expected to decrease with higher turbidity values. This concentration factor needs further analysis to determine if it has any significant effect in the water purification process and if so, if it can be used to increase the final efficiency.

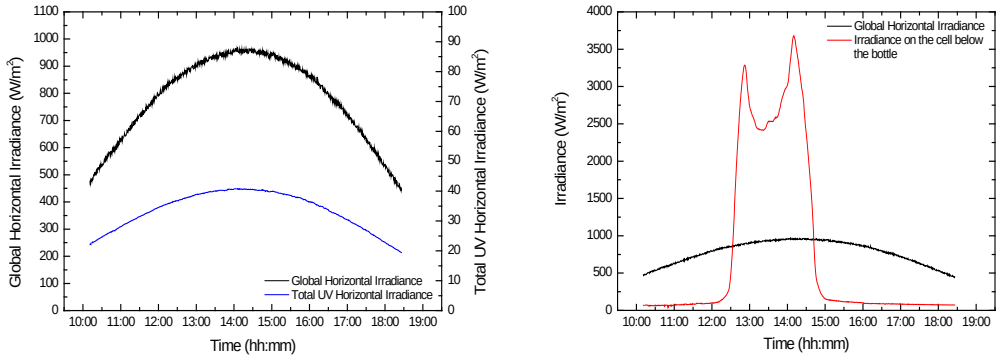

(a) (b)

Fig. 37: a) Climatic conditions during the experiment, including global horizontal irradiance and total UV irradiance; b) Irradiance on the cell below the bottle, showing a concentration effect that increases the irradiance during the central hours of the day (17th April 2013).

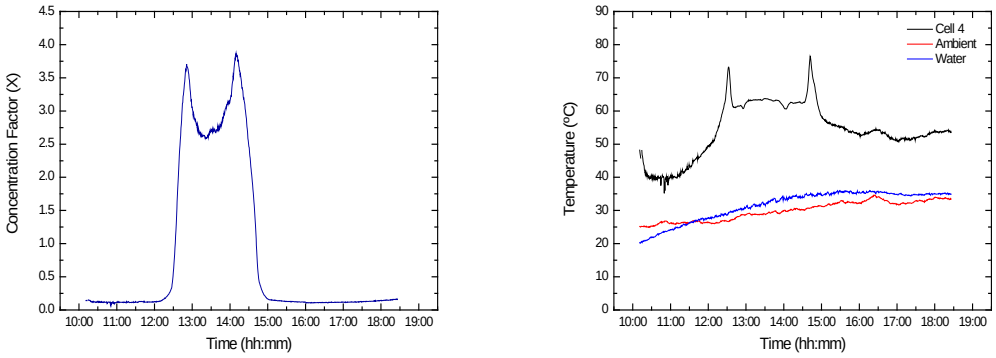

(a) (b)

Fig. 38: a) Concentration factor at the bottom of the bottle, up to 3.9X; b) Cell temperature, following the concentration effect; water temperature, increasing till 35ºC; and ambient temperature along the time of the experiment (17th April 2013).

5.4 Test with SODIS and polluted water

The last test used SODIS bottles to purify water polluted with a microorganism and evaluate the SolWat sensor performance by comparing the PV cells output with the water microbiological analysis. The final objective is to determine values or parameters of the PV sensor that provide relevant data about the water disinfection process.

A review on the main parameters of the solar disinfection process, including UV dose, global irradiance dose, water temperature, etc., was also conducted in order to identify the most appropriate parameter or combination of parameters to standardise the clean water detection on solar water purification.

5.4.1 Literature review on required dose for microorganisms inactivation under natural sunlight

It is required to know the main criteria for clean water in solar disinfection in order to develop a suitable sensor. In general, SODIS establishes the main criteria as a combination of time and weather parameters, consisting of 6h in a sunny day or between 2-3 days if it is cloudy. But being more specific implies studying the other main parameters: UV irradiance, global irradiance and water temperature, so we reviewed the main scientific literature on real sunlight water disinfection (not simulated light) in order to extract the main values of these parameters. This issue of determining the radiation required for

complete inactivation of microorganisms was already reported by Bandala et al. [15] in 2011 when developing clean water sensors for SODIS based on azo dyes.

This review is divided into three groups of pathogens that might be present in water: bacteria, viruses and protozoa. Table V summarises the main retrieved data from the different research studies. As we can observe, the group of the enteric bacteria is the most studied one, in comparison with the works conducted specifically with viruses or protozoa. The table gives three main parameters: UV dose, solar irradiation dose, and water temperature, not always provided or monitored at the same time in all the studies. Most of the works conducted under real sun used a system to control the water temperature, and only few of them allowed the temperature to follow the natural profile under the sun, which is more realistic when calculating inactivation rates and corresponding doses [46-50]. But the temperature-controlled experiments provide information about the effect of temperature and the calculation of doses of UV and global irradiance at different temperatures [51-52]. Overall, there is the feeling that only one parameter is not sufficient to define a clean water criteria when using solar disinfection and UV, but a combination of parameters including time, UV dose, global irradiance, water temperature; and their distributions along the day [48,5,53].

In general, the works show that the synergistic effects of temperature and UV are only relevant when the water temperature is over 45h [51]. Enteric bacteria and viruses require smaller doses of UV and global irradiance than protozoa (in these works, *Cryptosporidium parvum*), which are more resistant to solar disinfection. Another general observation is the no-regrowth of bacteria (*E. coli*) in the water treated naturally with sunlight during periods ranging from 5 days to 2 weeks after treatment. Finally, the comparison between UV doses and global irradiance between the different research works is really difficult due to the disparity of equipment used (varying in spectral ranges) and the different set-ups adopted in the experiments. However, it is necessary to analyse the studies and understand the main findings and the previous mentioned limitations to establish a clean water criteria for solar disinfection.

The first studies on solar water disinfection under real sun were conducted by Acra et al. [54] in 1984, when they tested water with enteric bacteria from both pure culture and real water in Pyrex flasks, giving times to 99.9% destruction on coliform bacteria and

E.coli but not UV dose nor global irradiance or temperature information. In following works they started to measure UV dose, finding similar values for *E. coli* and *Str. faecalis* [51]. In 1991, Wegelin et al. [51] in Switzerland continued with the research on solar disinfection and studied the required doses for inactivating the *E.coli* and *Str.faecalis* bacteria and the *Bacteriophage f2*, *Rotavirus* and *Encephalomyocarditis virus* viruses under real sun and with controlled temperature. The main findings were the synergistic effects of temperature and UV radiation for temperatures over 45ºC, increasing the inactivation rate of microorganisms; and the required dose for *E.coli*, 2000kJ/m^2 of solar radiation in the spectral range of 350nm-450nm, equivalent to 5h of mid-latitude midday summer sunshine in Switzerland. This value, increased to one more hour, is the one used by EAWAG (Swiss Federal Institute of Aquatic Science and Technology) in the dissemination of SODIS technology around the world [53]. Inactivation doses for the analysed viruses were similar except for the *Encephalomyocarditis virus* that was approximately double. *Vibrio cholerae* was first studied under real sun by Sommer et al. in 1997 [46], using transparent plastic bags instead of plastic bottles. In principle, bags are more effective than bottles because their reduced water depth, but they are also less manageable and reliable in developing regions. Dose for 99.9% inactivation was 195kJ/m^2 of UVA radiation.

In 2006 and 2008, Berney et al. [52] and Boyle et al. [47] respectively, conducted a thorough group of tests each, the former with quartz containers and controlled temperature at 37ºC, and the latter with PET bottles and natural profile temperature. Berney et al. obtained inactivation doses of 1530kJ/m^2 (350-450nm) for *E. coli*, 2431kJ/m^2 (350-450nm) for *Salmonella enteric serovar Typhimurium*, 1194 kJ/m^2 (350-450nm) for *Shigella flexneri*, and 305kJ/m^2 (350-450nm) for *Vibrio cholerae*. These values were in agreement with the previous published works, as they are between the doses calculated for temperatures of 20ºC and 50ºC by Wegelin et al. The work from Boyle et al. represents the first detailed study using PET bottles with natural temperature. They analysed the solar disinfection process for *E.coli* and *S. epidermidis* as well as for two other bacteria that were not studied before: *C. jejuni* and *Y. enterocolitica*. Both bacteria were also inactivated by solar disinfection, although *Y. enterocolitica* was more resistant than the other bacteria.

Finally, in 2012, Marques et. al [50] conducted different tests along the year with water from a polluted river, analysing thermotolerant coliform bacteria and *E. coli*. They

achieved complete inactivation for a cumulative global irradiance of 9776kJ/m^2 (full spectrum), with water temperature above 45ºC for at least 5h.

The most recent review on SODIS technology has been written by McGuigan et al. [5] in 2012, giving a summary of the waterborne microbial species that are now known to be inactivated by SODIS, showing how there is limited work done with viruses and protozoa. Only the works from Méndez-Hermida et al. in 2007 [48] and Gómez-Couso et al. in 2009 [49] have analysed under real sunlight the solar inactivation of *Cryptosporidium parvum* oocysts, with much higher UV dose required than for enteric bacteria or viruses.

Table V: Main waterborne pathogens (bacteria, viruses and protozoa) and their inactivation parameters (UV, solar irradiation, temperature) under natural sunlight from different studies.

Enteric bacteria

Microorganism	Container	Microorganism source	Initial microorganism density (CFU/ml)	Time to 99.9% (min)	UV dose required (kJ/m^2)	Solar irradiation required (kJ/m^2)	Temperature (°C)	Reference	Year
Coliform bacteria	Pyrex	Real water	--	85	--	--	--	Acra et. al	1984
Coliform bacteria	Pyrex	Pure culture	--	80	--	--	--		
E. coli	Pyrex	Pure culture	--	75	--	--	--		
P. aerugenosa	Pyrex	Pure culture	--	15	--	--	--		
S. flexneri	Pyrex	Pure culture	--	30	--	--	--		
S. typhi	Pyrex	Pure culture	--	60	--	--	--		
S. enteritidis	Pyrex	Pure culture	--	60	--	--	--		
S. paratyphi B	Pyrex	Pure culture	--	90	--	--	--		
E. coli	Quartz	Pure culture	10^3-10^4	--	306 (320-405nm)	2040 (350-450nm) 15.5MJ/m^2 (400-1100nm)	20	Wegelin et al.	1994
E. coli	Quartz	Pure culture	10^2-10^7	--	78 (320-405nm)	520 (350-450nm) 4MJ/m^2 (400-1100nm)	50		
E. coli	Quartz	Real water	10^2-10^7	--	285 (320-405nm)	1900 (350-450nm) 14.4MJ/m^2 (400-1100nm)	20		
E. coli	Quartz	Real water	10^2-10^7	--	75 (320-405nm)	500 (350-450nm) 3.8MJ/m^2 (400-1100nm)	50		
Str. faecalis	Quartz	Pure culture	10^4	--	209 (320-405nm)	1390 (350-450nm) 10.6MJ/m^2 (400-1100nm)	20		
Vibrio cholerae	Plastic bag	Pure culture	10^4	140	195	--	max reached 55°C natural temperature	Sommer et al.	1997
E. coli	PET	Real water	--	--	--	9MJ/m^2	30	SODIS manual	2002
E. coli	PET	Real water	--	--	--	1.8MJ/m^2	50		
E. coli	Quartz	Pure culture	10^7	182 (90%)	230 (320-405nm)	1530 (350-450nm) 11.6MJ/m^2 (400-1100nm)	37	Berney et al.	2006
Salmonella enterica serovar T	Quartz	Pure culture	10^7	187 (90%)	365 (320-405nm)	2431 (350-450nm) 18.5MJ/m^2 (400-1100nm)	37		
Shigella flexneri	Quartz	Pure culture	10^7	136 (90%)	179 (320-405nm)	1194 (350-450nm) 9.1MJ/m^2 (400-1100nm)	37		
Vibrio cholerae	Quartz	Pure culture	10^7	24 (90%)	46 (320-405nm)	305 (350-450nm) 2.3MJ/m^2 (400-1100nm)	37		
Campylobacter jejuni	PET	Pure culture	10^6	2.1 (90%)	14.5 (295-385nm)	2 days exposure, 8h each, 30.6MJ/m^2 average per day	natural temperature	Boyle et al.	2008
Yersinia enterocolitica	PET	Pure culture	10^6	78.6 (90%)	89.9 (295-385nm)	2 days exposure, 8h each, 30.6MJ/m^2 average per day	natural temperature		
E. coli	PET	Pure culture	10^6	33.4 (90%)	125.6 (295-385nm)	2 days exposure, 8h each, 30.6MJ/m^2 average per day	natural temperature		
Staphylococcus epidermidis	PET	Pure culture	10^6	12 (90%)	52.9 (295-385nm)	2 days exposure, 8h each, 30.6MJ/m^2 average per day	natural temperature		
E. coli	PET	Real water	--	--	--	9.78MJ/m^2	above 45°C for 5h natural	Marques et al.	2013

Viruses

Microorganism	Container	Microorganism source	Initial microorganism density (CFU/ml)	Time to 99.9% (min)	UV dose required (kJ/m^2)	Solar irradiation required (kJ/m^2)	Temperature (°C)	Reference	Year
Bacteriophage f2	Quartz	Pure culture	10^4-10^{10}	--	321 (320-405nm)	2140 (350-450nm) 16.3MJ/m^2 (400-1100nm)	30	Wegelin et al.	1994
Rotavirus	Quartz	Pure culture	10^4-10^{10}	--	372 (320-405nm)	2480 (350-450nm) 18.9MJ/m^2 (400-1100nm)	30		
Encephalomyocarditis virus	Quartz	Pure culture	10^4-10^{10}	--	--	~ double dose	30		

Protozoa

Microorganism	Container	Microorganism source	Initial microorganism density (oocysts/ml)	Time to 99.9% (min)	UV dose required (kJ/m2)	Solar irradiation required (kJ/m2)	Temperature (°C)	Reference	Year
C. parvum	Glass	Pure culture	--	--	--	37-50MJ/m^2	natural temperature	Méndez-Hermida et al.	2007
C. parvum	Glass with CPC (1X, 1.89X)	Natural	10^6	--	731.5 (6h, 5% viability)	--	temperature max temp 1X - 42 max temp 1.89X - 50.7	Gómez-Couso et al.	2009

From all the findings from the reviewed works in Table V and considering the criteria given in the SODIS manual [53], we propose a combination of parameters measured by the SolWat sensor to decide when the water is clean. We establish the limits so most of the inactivation doses for both enteric bacteria and viruses are covered. These are the **proposed clean water criteria for the SolWat sensor** when the water turbidity is below 30NTU:

- Sunshine duration > 6h.
- Cumulative global irradiation with water temperature above 30ºC > 9MJ/m^2.
- Cumulative global irradiation with water temperature above 30ºC at the bottom of the bottle > 4.5 MJ/m^2.
- Cumulative UV with temperature above 30ºC > 375kJ/m^2.

5.4.2 Preliminary test with SODIS bottles and *E. coli*

After the literature review, a preliminary test was conducted with a real microorganism in the water, *E.coli*, to test the suitability of the SolWat sensor. The test was conducted at the facilities of IMDEA Agua (Alcalá de Henares, Spain).

The *E.coli* used was provided by IMDEA Agua, and was previously isolated from wastewater. 1mL of the bacterial cell preparation was added to a 1,500mL SODIS PET bottle rinsed and disinfected and then filled with filtered Milli-Q water (0.22µm). The bottle was prepared following SODIS guidelines, first filling up to 75% of capacity, then shaking for 20s, and finally filling up completely. A total of 8 bottles were prepared, 6 for the sunlight exposure (one per hour), and 2 for control (one in the lab and one outdoor in the shade).

The SODIS bottles were set up N-S oriented under natural sunlight for 6 hours along with the SolWat sensor monitoring global irradiance, UV irradiance, irradiance under the bottle and cell 4 and water temperature in the lid, plus a small weather station measuring global horizontal irradiance, UV irradiance and ambient temperature (Fig. 39). Data were recorded automatically at 30s-intervals. Each hour, one bottle was removed for microbiological analysis.

Microbiological analysis was conducted filtering the samples through a membrane filter of 0.45µm. The samples were previously diluted if necessary to obtain between 20 and 200 colonies per filter, with dilution factors up to 10^4 using filtered Milli-Q water. Each sample was filtered three times and then transferred to a plate with a Chromogenic Coliforms Agent (CCA, Scharlau 1-695) prepared with the Coliform CV Selective Supplement (Scharlau). Plates were incubated at 37ºC for 18-24h and after plate counts were determined, enumerating *E.coli* as deep blue to violet colonies (CFU/100mL).

(a) (b)

Fig. 39: Set-up of experiment with PET bottles filled with water with *E.coli* and the SolWat sensor unit 2 underneath one of them to measure irradiance in the bottom of the bottle and water temperature, along with the SolWat sensor unit 1 measuring sunshine duration, global irradiance and UV irradiance; and a weather station (21st May 2013).

Climatic conditions during the experiment are shown in Fig. 40a, showing the global irradiance and the UV irradiance in the horizontal plane. Overall, it was a sunny day but windy, with fast clouds passing-by and dropping the irradiance to low levels each time that a cloud crossed the sun (corresponding to multiple spikes in the global and UV irradiance). From the SolWat sensor, Fig.40b shows the irradiance below the bottle in comparison with the global irradiance. As in the experiment 5.3, we can observe the concentration factor on the cell, although this time it is lower due to the different orientation of the bottle. Despite being north-south as in the 5.3 experiment, the bottle lid is at the northern side instead of the southern side, so the shape of the bottle neck might have different concentration effect on the cell. Fig. 41a shows a detail of the concentration factor, up to 1.86X.

Regarding temperatures (Fig. 41b), we observe that the ambient temperature was of 20ºC on average, varying due to a very windy day with cool air. The solar cell temperature was about 15ºC above ambient temperature, but it does not follow the concentration profile due to the fast clouds passing by, so the thermal inertia of the cell cannot follow the rapid changes. Finally, the water temperature of the bottle with the sensor was of 24ºC on average, not reaching 30ºC at any moment. The observed peak is probably caused by concentration effects. During this experiment the temperature sensor inside the bottle is facing south, so it is not protected from concentration effects within the bottle, reaching at a certain moment a peak concentration that reaches almost 100ºC. Although the thermocouple would tolerate the high temperature, it is a better practice to change the orientation of the bottle and put the lid in the opposite direction so the thermocouple is protected under the shade and does not lead to false water temperatures.

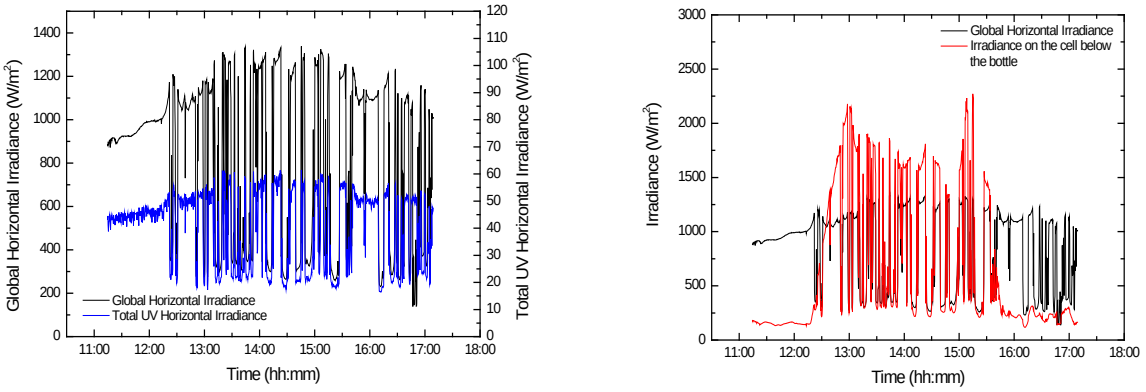

(a) (b)

Fig. 40: a) Climatic conditions during the experiment, including global horizontal irradiance and total UV irradiance; b) Irradiance on the cell below the bottle, showing a concentration effect that increases the irradiance during the central hours of the day (21st May 2013).

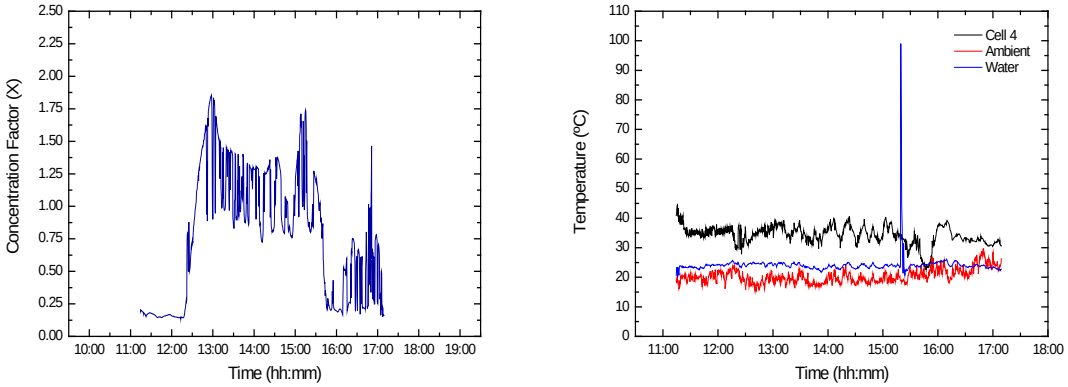

(a) (b)

Fig. 41: a) Concentration factor at the bottom of the bottle, up to 1.9X; b) Cell temperature, above 15ºC of ambient temperature and water temperature, with a peak due to concentration directly onto the sensor, over the span of the experiment (21st May 2013).

Fig. 42 presents the results corresponding to the microbiological analysis of the SODIS bottles exposed to the real sun and the control samples kept in the dark. We observe how the E.coli is being inactivated, reducing the bacteria population with solar exposure. The sample corresponding to the 6th hour presents an increase in bacterial population, possibly due to different exposure conditions as it is the only bottle not directly on the ground but over the SolWat sensor, more exposed to the wind and with less reflected irradiance from the ground, leading to reduced temperature and reduced irradiance exposure. A slower inactivation would explain this different result. Other possible causes would be re-growth of bacteria but it would be unlikely due to the same climatic conditions. More work should be done on this issue to determine the cause of the difference, measuring in future experiments the water temperature of the other bottles and using two bottles for the last hour, one on the ground and one in the sensor. After 5h under natural sunlight, the reduction of *E.coli* in the ground bottles is of 96%.

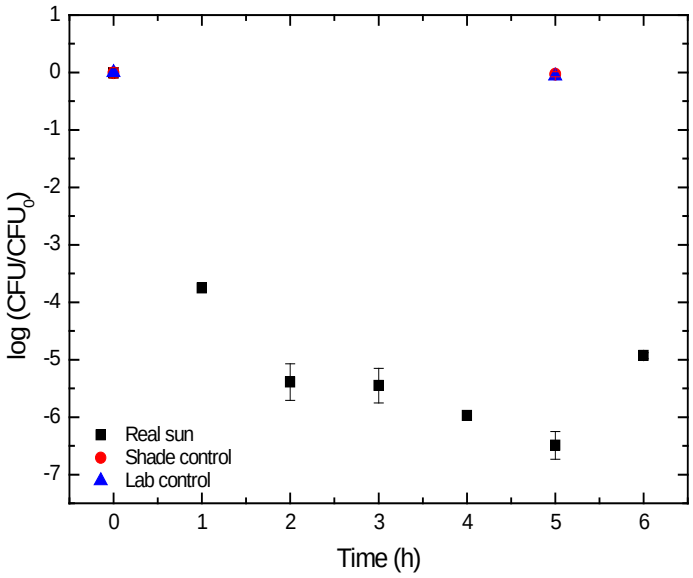

Fig. 42: Inactivation curves of *E.coli* under natural sunlight in log reduction units, showing reduction in bacteria population with increased solar exposure (21st May 2013). Sample corresponding to the 6th hour presents an increase in bacterial population, possibly due to different exposure conditions as it is the only bottle not directly on the ground but over the SolWat sensor, more exposed to the wind and with less reflected irradiance from the ground, leading to reduced temperature and reduced irradiance exposure. Control samples, both in the lab and in the shade outdoor, do not show inactivation. Error bars represent triplicate measurement.

Finally, from the SolWat sensor monitored data, we calculated the parameters required to decide if the water is clean or not according to the proposed criteria for clean water detection. Table VI shows the obtained parameters against the proposed criteria, where none of the clean water criteria values are met. Fig. 42 shows the different cumulative values of the parameters along time. Sunshine duration achieves roughly 5h due to the fast clouds, while cumulative global irradiation is of 17.3MJ/m^2, cumulative global irradiation is of 13.4MJ/m^2 and cumulative UV is of 528kJ/m^2, but all below 30ºC water temperature. With these data, the decision would be of '**no clean water**', which agrees with the microbiological data. However, it would be necessary to conduct extensive experiments to validate the proposed criteria, and it would be also interesting to establish a new set of clean water criteria using the same parameters but for the case of low temperatures.

Table VI: Proposed clean water criteria based on sunshine duration, global irradiation, global irradiation through the bottle and UV irradiation; and calculated values for the conducted experiment (21st May 2013), not meeting the criteria for clean water.

Parameter	Clean Water Criteria	Experiment 21th May 2013
Sunhine duration	> 6h	5.08
Cumulative global irradiation with water temperature above 30°C	> 9MJ/m^2	0
Cumulative global irradiation with water temperature above 30°C at the bottom of the bottle	> 4.5 MJ/m^2	0
Cumulative UV with temperature above 30°C	> 375kJ/m^2	0
Cumulative global irradiation	--	17.3 MJ/m^2
Cumulative global irradiation at the bottom of the bottle	--	13.4 MJ/m^2
Cumulative UV	--	528 kJ/m^2

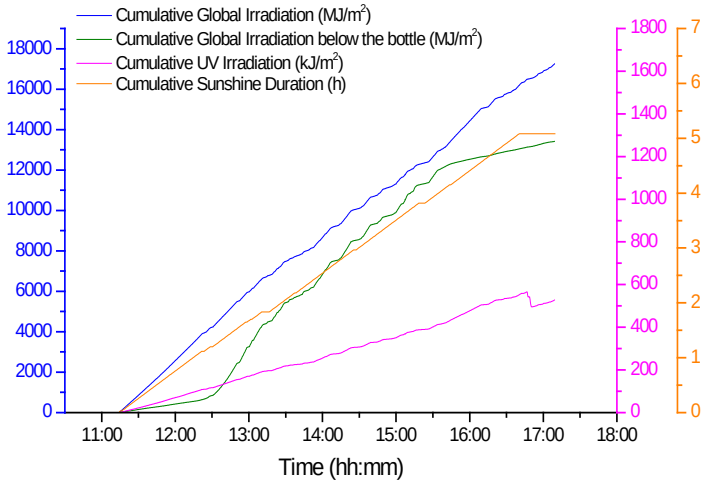

Fig. 43: Cumulative values of sunshine duration, global irradiation, global irradiation under the bottle and cumulative UV measured by the SolWat sensor during the SODIS experiment with *E.coli* (21st May 2013).

In summary, the low-cost SolWat sensor is capable of monitoring several parameters relevant to SODIS, including sunshine duration, global irradiation, water temperature and UV irradiation, plus an additional parameter which is the irradiance through the bottle. This set of information can be used to determine whether the water is clean or not after the solar disinfection according to a proposed criteria that has to be further analysed, improved and validated.

6. CONCLUSIONS AND FUTURE WORK

A new low-cost clean water sensor based on photovoltaic solar cells has been developed for addressing one of the problems related to the low reliability of solar water technologies in developing countries. One of the main issues when using solar water disinfection with UV or solar water pasteurization is that the user does not know when the water is clean and safe to drink. Solar cells are currently inexpensive and reliable, and they provide information about received irradiation and temperature based on their main characteristics: current and voltage, with are directly proportional to irradiance and temperature.

The potential of solar cells as clean water sensors for solar water technologies was explored in Chapter 2, presenting also the main requirements of the low-cost sensor for each of the technologies. Main parameters were identified as global irradiation, UV irradiation, sunshine duration and water temperature. Solar cells are known to measure global irradiance and temperature, but no information was found on sunshine hours, so it was required a detailed analysis to study if the solar cells could serve as sunshine duration sensors accurately following the WMO standards. Chapter 3 was dedicated to this objective, implementing the approved algorithms for pyranometers in solar cells and conducting a comparison of results between the SD calculated by the solar cell, the pyranometer and the pyrheliometer (reference). 1-year dataset from the University of Cyprus was used, and three pyranometric algorithms were implemented: the Slob and Monna, the Hinssen and Knap and the Olivieri method. The algorithms were adapted to the tilted pyranometer and calibrated photovoltaic silicon solar cell from Cyprus. Main conclusions were that all the algorithms underestimated sunshine duration over the span of a year and the results between the pyranometer and the solar cell were comparable.

In Chapter 4 we presented a design of the clean water PV sensor for SODIS bottles, along with the materials, manufacturing and initial charaterisation. The main parameter, sunshine duration, was already proven to be measurable by a solar cell. The other important parameter was the UV irradiance, which was designed to be measured by two-identical solar cells, one of them with a UV-blocking filter on top, so the total UV irradiance could be calculated as the difference between the two solar cells output. The first cell would be measuring UV-VIS-NIR and the second only VIS-NIR. The UV filter

material was explored and a low-cost architectural film was selected. A second pair of solar cells were designed to be under the bottle, the first measuring the irradiance through the bottle and the second temperature, although this temperature would not be representative of the water temperature as the thermal mass of the cell is too small I n comparison to the full water volume in this particular application. A low cost thermocouple was introduced in the lid of the bottle, insulating by silicone for its use in water measurement. Manufacturing process was described in detail and initial calibration followed the international standards for photovoltaic solar cells.

Finally, Chapter 5 was dedicated to the different tests conducted under real sun with SODIS technology to characterise the sensor performance. The objective of these tests was to determine if the new sensor provides useful data to help the water quality monitoring. More specifically, we studied the following parameters measured by the solar cells: sunshine duration, total global irradiance and irradiance at the bottom of the bottle, UV irradiance and water temperature. Characterisation as sunshine duration sensor and global irradiance was conducted, verifying that the SolWat sensor can be used to measure both global horizontal irradiance and sunshine duration. Regarding the UV irradiance measurement, we found several issues with the attachment of the UV film to the cell, which were almost resolved by attaching the film directly onto the cell. Initial tests showed good correlation between the UV calculated by the solar cells and the UV reference measured by a commercial UV sensor. On the other hand, this type of UV films could be even a better solution than an expensive UV sensor as their main material is PET, the same as the SODIS bottles, and so they measured the UV that is really available to the water in the bottle for the solar disinfection.

Finally, the irradiance through the bottle showed that when the water is clean, during the central hours of the day, the bottle and the water might act as a lens, concentrating the solar radiation into a smaller area. This might mean that the circular shape of the bottle is actually transmitting most of the light during the concentration effect and not absorbing it, which can have two different effects in the water purification process. First, we could think that this effect would accelerate the process, as it seems that we get more light to the bottom of the bottle. But this means that the sunlight is not being absorbed through the bottle, so the first layers of water might not being affected by the UV disinfection, so it might be the opposite effect, and it decreases the rate of inactivation. On

the other hand, the concentration is accumulating solar irradiance in a smaller area, which will heat up faster. This heat could be transferred by conduction to the rest of the bottle and contribute to increase the water temperature, improving the water disinfection.

After all these tests studying the different parameters, a real test with water containing *E.coli* was conducted to evaluate the SolWat sensor performance by comparing the PV cells output with the water microbiological analysis. The final objective was to determine values or parameters of the PV sensor that provide relevant data about the water disinfection process. The PET bottles were exposed for a total of 6h and all the main parameters were recorded by the SolWat sensor. Prior to the experiment, a review on the main parameters of the solar disinfection process, including UV dose, global irradiance dose, water temperature, etc., was also conducted to identify the most appropriate parameter or combination of parameters to standardise the clean water detection on solar water purification, and a first proposal of clean water criteria based on this information was given. For this preliminary experiment, the bacteria were not fully inactivated but the population decreased to a 96%. The SolWat sensor was capable of monitoring the parameters relevant to SODIS, including sunshine duration, global irradiation, water temperature and UV irradiation, plus the irradiance through the bottle. This set of information was used to determine whether the water is clean or not after the solar disinfection according to the proposed criteria and in this particular case the sensor data were in agreement with the microbiological analysis, but it is only a preliminary experiment and therefore further work needs to be conducted and the SolWat sensor and the clean water criteria must be analysed, improved and validated.

From these findings, and in closer inspection of the data, we can identify different areas were future research should focus. The first one should be to solve the attachment of the UV film to the cell, and considering the possibility of using larger cells for the differential sensor so the errors can be minimize. This would not be a significant increase in cost. On the other hand, the UV film used was 95% UV-blocking, but there are 99% UV-blocking filters that could improve the performance of the sensor at a low cost, with less than 14€/m^2 for small quantities (for larger orders the cost would decrease).

The effect of the concentration should be further investigated in order to understand the possible advantages or limitations. It might be interesting to combine this concentration

effect with other concentration methods already well-proven such as aluminium foils in half of the bottles or half-black bottles to increase temperature. Orientation of the bottle should be also studied to determine if it has any effect on the concentration or not. Turbid waters would not present this effect and or waters with a large number of bacteria might act as a colloid and not present concentration effect either.

Proposed clean water criteria using the SolWat main parameters should be validated and/or optimised or modified according with the experimental findings. Lower temperatures and different microorganisms might be also considered.

Finally, cost and reliability should be fully explored. One of the main issues of the sensors, although inexpensive (solar cells can be as low as 0.1€/cell), is the data monitoring, i.e., that a low cost datalogger is also required. This is already being investigated in collaboration with the University of Jaén, where a low-cost datalogger with high-resolution has been already developed using Arduino, with a total cost of the first prototype of only 60€ (equivalent commercial dataloggers can be up to 3,000€).

7. REFERENCES

1. WHO-Unicef JMP, update on 'Progress on Drinking Water and Sanitation', 2012.

2. S. Loo et al., Emergency water supply: a review of potential technologies and selection criteria, *Water Research* 46 (2012), pp. 3125-3151.

3. D. M. Johnson et al., Feasibility of water purification technology in rural areas of developing countries, *Journal of Environmental Management* 88 (2008), pp. 416-427.

4. WHO, 'Guidelines for drinking-water quality', 4th edition, 2011.

5. K. G. McGuigan et al., 'Solar Water Disinfection (SODIS): A Review from Bench-top to Roof-top', *Journal of Hazardous Materials* 235-236 (2012), pp. 29-46.

6. C. Ray, R. Jain (eds.), *Drinking Water Treatment*, Strategies for Sustainability, 2011, Springer, New York.

7. M. Boyle et al, Bactericidal effect of solar water disinfection under real sunlight conditions, *Applied and Environmental Microbiology* 74, No. 10 (2008), 2997-3001.

8. K. Nakata et al., Photoenergy conversion with TiO2 photocatalysis: New materials and recent applications, *Electrochimica Acta* (2012), In Press, http://dx.doi.org/10.1016/j.electacta.2012.03.035.

9. M. N. Chong et al., Recent developments in photocatalytic water treatment technology: A review, *Water Research* 44 (2010), 2997-3027.

10. M. Pelaez et al., A review on the visible light active titanium dioxide photocatalysts for environmental applications, *Applied Catalysis B: Environmental* 125 (2012), pp. 331–349.

11. L. Pastrana-Rodriguez et al., Advanced nanostructured photocatalysts based on reduced graphene oxide–TiO_2 composites for degradation of diphenhydramine pharmaceutical and methyl orange dye, *Applied Catalysis B: Environmental* 123-124 (2012), pp. 241–256.

12. M. Vivar et al., A Concept for a Hybrid Solar Water Purification and Photovoltaic System, *Solar Energy Materials and Solar Cells* 94 (2010) 1772-1782.

13. M. Fuentes et al., Results from a first autonomous optically adapted photocatalytic-photovoltaic module for water purification, *Solar Energy Materials and Solar Cells* 100 (2012), pp. 216-225.

14. R. Copperwhite, C. McDonagh and S. O'Driscoll, A camera phone-based UV-dosimeter for monitoring the solar disinfection (SODIS) of water', *IEEE Sensors Journal* 12 (2012), pp.1425-1426.

15. E. R. Bandala et al., 'Application of azo dyes as dosimetric indicators for enhanced photocatalytic solar disinfection (ENPHOSODIS)', *Journal of Photochemistry and Photobiology A: Chemistry* 218 (2011), pp. 185-191.
16. J. A. Byrne et al., 'Photocatalytic Enhancement for Solar Disinfection of Water: A Review', *International Journal of Photoenergy* Volume 2011 (2011), Article ID 798051, 12 pages.
17. R.H. Metcalf, 'The Microbiology of Solar Water Pasteurization, with Applications in East Africa'. Sacramento, California State University, 2006. (accessed 17 January 2013).
18. International Standard IEC 61215: 'Crystalline silicon terrestrial photovoltaic (PV) modules. Design qualification and approval'.
19. PV Education, http://www.pveducation.org, accessed 30th January 2013.
20. Isofotón, http://www.isofoton.es, accessed 30th January 2013.
21. 'Solar Energy Technologies' lectures corresponding to Photovoltaic Systems, Bachelor of Engineering degree, College of Engineering, Australian National University, 2010.
22. 'Energía Solar Fotovoltaica – Sistemas de Concentración', Instituto de Sistemas Fotovoltaicos de Concentración (ISFOC), Puertollano, Spain, 2007.
23. International Standard IEC 60904-5: 'Photovoltaic Devices. Part 5. Determination of the equivalent cell temperature (ECT) of photovoltaic (PV) devices by the open-circuit voltage method'.
24. M. Wegelin et al., 'Solar water disinfection: Scope of the process and Analysis of radiation experiments', *Journal Water SRT – Aqua* Vol. 43 Nº 3 (1994), pp. 154-169.
25. 'Measurement of Sunshine Duration. Part I: Measurement of Meteorological Variables', World Meteorological Organisation (WMO), Guide to Meteorological Instruments and Methods of Observation, 8th Ed, Secretariat of the World Meteorological Organisation, 2008, Update 2010.
26. J. M. Burgos, 'Detector de purificación de agua mediante SOLWAT', honours project, Departamento de Ingeniería Electrónica y Automática, Universidad de Jaén, 2013.
27. M. Paulescu et al., 'UV Solar Irradiance From Broadband Radiation and Other Meteorological Data', *Atmospheric Research* 96 (2010), pp. 141-148.
28. Y. B.L. Hinssen and W. H. Knap, 'Comparison of Pyranometric and Pyrheliometric Methods for the Determination of Sunshine Duration', *Journal of Atmospheric and Ocean Technology* 24 (2007), pp. 835-846.

29. E. Vuerich et al.,'Updating and Development of Methods for Worldwide Accurate Measurements of Sunshine Duration', TECO-2012, Brussels, Belgium, 16-18 October 2012.
30. F. Massen,' Sunshine duration from pyranometer readings', Meteorological Station of the Lycée classique de Diekirch, Luxembourg, 2011, 22pp.
31. Flickr User Laurent KB, http://www.flickr.com/photos/laurentis/1694572774/, accessed 5th March 2013.
32. Image from Wikimedia, http://upload.wikimedia.org/wikipedia/commons/6/65/Sunshine_card_closeup.JPG , accessed 5th March 2013.
33. Kipp&Zonen, http://kippandzonen.com, accessed 5th March 2013.
34. Y. B. L. Hinssen, 'Comparison of different methods for the determination of sunshine duration', KNMI Scientific Rep WR-2006-06, 72pp.
35. N. H. Reich et al.,'Performance ratio revisited: is PR > 90% realistic?', *Progress in Photovoltaics: Research and Applications* 20 (2012), pp. 717–726.
36. International Standard IEC 60904-Part 2: 'Requirements for reference solar cells'.
37. J. Meydbray, K. Emery and S. Kurtz, 'Pyranometers and Reference Cells, What´s the Difference?' NREL Journal Article, April 2012, 7pp.
38. H. Haeberlin et al., 'Comparison of Pyranometer and Si-Reference cell solar irradiation data in long term PV plant monitoring', *13th EU PV Conference on Photovoltaic Energy Conversion*, Nice, France, 1995.
39. L. Dunn, M. Gostein and K. Emery, "Comparison of Pyranometers vs. Reference Cells for Evaluation of PV Array Performance," *Proceedings of the 38th IEEE Photovoltaic Specialists Conference (PVSC)*, Austin, TX, June 3-8, 2012.
40. J. Meydbray et al., 'Pyranometers and Reference Cells, What Makes the Most Sense for PV Power Plants?' NREL Journal Article, October 2012, 12pp.
41. M. Lundqvist, C. Helmke and H.A. Ossenbrink, 'ESTI-LOG PV Plant Monitoring System', *Solar Energy Materials and Solar Cells* 47 (1997) pp. 289-294.
42. M. Vivar et al., 'First Lab-scale Experimental Results from a Hybrid Solar Water Purification and Photovoltaic System', *Solar Energy Materials and Solar Cells* 98 (2012) pp. 260-266.
43. 'Renewable Energy Applications for Freshwater Production', Edited by J. Bundschuh and J. Hoinkis, IWA Publishing, CRC Press, Taylor and Francis group, London, UK, 2012.

44. SCL SR PS4 Llumar film technical datasheet, provided by Impersol Lda (www.impersol.pt), 2013.
45. SCL SR PS4 Llumar film reference installation guide, provided by Impersol Lda, 2013.
46. B. Sommer et al., 'SODIS – An Emerging Water Treatment Process', *J Water SRT-Aqua* 46 (1997), Nº 3, pp. 127-137.
47. M. Boyle et al., 'Bactericidal Effect of Solar Water Disinfection under Real Sunlight Conditions', *Applied and Environmental Microbiology* 74 (2008), Nº10, pp. 2997–3001.
48. F. Méndez-Hermida et al., 'Disinfection of Drinking Water Contaminated with Cryptosporidium parvum oocysts under Natural Sunlight and Using the Photocatalyst TiO_2', *Journal of Photochemistry and Photobiology B: Biology* 88 (2007), Issues 2–3, pp. 105-111.
49. H. Gómez-Couso et al., 'Effect of the Radiation Intensity, Water Turbidity and Exposure Time on the Survival of Cryptosporidium during Simulated Solar Disinfection of Drinking Water', *Acta Tropica* 112 (2009), Issue 1, pp. 43-48.
50. A. R. Marques et al, 'Efficiency of PET Reactors in Solar Water Disinfection for Use in Southeastern Brazil', *Solar Energy* 87 (2013), pp. 158-167.
51. M. Wegelin et al., 'Solar Water Disinfection: Scope of the Process and Analysis of Radiation Experiments', *J Water SRT-Aqua* 43 (1994), Nº 3, pp. 154-169.
52. M. Berney et al., 'Efficacy of Solar Disinfection of Escherichia coli, Shigella flexneri, Salmonella Typhimurium and Vibrio cholerae', *Journal of Applied Microbiology* 101 (2006), Nº 4, pp. 828-836.
53. 'Solar Water Disinfection – A Guide for the Application of SODIS', SANDEC, Eawag, Duebendorf, 2002.
54. A. Acra, Z. Raffoul and Y. Karahagopian, 'Solar Disinfection of Drinking Water and Oral Rehydration Solutions: Guidelines for Household Application in Developing Countries', Publisher Illustrated Publications for UNICEF, Paris, 1984.

8. ANNEXES

8.1 Medida de I_{SC} de células cortadas bajo condiciones estándar de medida (1 sol, 25ºC) utilizando el simulador solar IES-UPM, espectro AM1.5G.

Célula	Isc a 1 sol (mA)
12b-17	64,2
15	64,2
11-2-17	64,2
11b-17	64
17b	64
7b-17	63,9
16-18	63,9
6-16	63,8
9-dedos	63,8
14b-17	63,8
12-2	63,8
11	63,7
13	63,7
11-2-b	63,7
9	63,6
18b	63,6
3b-17	63,5
10	63,5
12-2b-17	63,5
7	63,4
20b	63,4
12	63,3
16b	63,3
2b-13	63,2
4	63,2
5-17	63,2
5b	63,2
6b	63,2
14	63
15b-1	63
18-4	63
19b	63
13b-17	62,9
3	62,8
17-3	62,8
20-6	62,8
1	62,4
19-5	62,3
1b-17	62,2
4b-17	62,1
10b-17	61,6
2	61,2
8	61,2

8.2 MATLAB code programmed for the sunshine duration algorithms

Main functions including general algorithms and basic functions, not including modifications for tilted surfaces neither procedures to work with specific data.

```
%************* Calculate_day_number function ********************
%
% Calculate_day_number
%
% Function that calculates the day number for an specific date and time.
% Inputs:date_time (num).
%
% Marta Vivar, 12/02/2013
%
%*************************************************************************
**

function [dn]= Calculate_day_number (date_time)


% calculate day number

date_time_vec = datevec(date_time);

year = date_time_vec(1);
month = date_time_vec(2);
day = date_time_vec(3);

date=[year,month,day];
date_num=datenum(date);

year_ref = year-1;
start_year_str = [year_ref,12,31];
start_year= datenum(start_year_str);

dn=date_num-start_year;

end
```

```
%************* Calculate_sun_elevation_angle function ******************
%
% Calculate_sun_elevation_angle
%
% Function that calculates the sun elevation angle for an specific
location
% and date and time. Inputs:date_time, latitude,longitude,dif_time,
% summer advance.
%
% Marta Vivar, 12/02/2013
%
%
%
%*********************************************************************
**

function [Sun_elevation_angle]= Calculate_sun_elevation_angle
(date_time,latitude,longitude,dif_GMT,summer_advance)

Sun_elevation_angle = 0; %Initialise sun elevation angle to zero
declination = 0;
dn = 0;
light_savings = 0;

% calculate day number

date_time_vec = datevec(date_time);

year = date_time_vec(1);
month = date_time_vec(2);
day = date_time_vec(3);

date=[year,month,day];
date_num=datenum(date);

hour = date_time_vec(4);
min = date_time_vec(5);
sec = date_time_vec(6);

% Local standard time
time=[hour,min,sec];
time_num=time(1)+time(2)/60+time(3)/3600;

year_ref = year-1;
start_year_str = [year_ref,12,31];
start_year= datenum(start_year_str);

dn=date_num-start_year;

% calculate declination

declination = 23.45 * sind ((360/365) * (dn+284));


% ** Start calculation of hour angle w **

%Equation of Time (in min)
```

```
B = (360/365)*(dn-81);

EOT =(9.87*sind(2*B))-(7.53*cosd(B))-1.5*sind(B);

% Local Standard Meridian Time LSMT (in degrees)

long_standard_m = 15*(dif_GMT);%Difference of local time with GMT -
Greenwich


% Time Correction Factor (in min)

TC = 4*(long_standard_m-longitude)+EOT;

% Consider light savings in summer
if summer_advance == 1
    if 84<dn<301 % 28 oct 2011 end light saving, 25 march 2012 begins
        light_savings=1;
    else
        light_savings=0;
    end
end

% Solar Time (in hours)

ST = time_num + (TC/60)-light_savings;

% Hour angle w (in degrees)

w = 15*(ST-12);

% ** Finish calculation hour angle w **


% calculate sun elevation angle

Sun_elevation_angle =
asind(((sind(declination))*(sind(latitude)))+((cosd(declination))*(cosd(l
atitude))*(cosd(w))));


end
```

```
%************* Calculate_azimuth function ********************
%
%
% Marta Vivar, 12/02/2013
%
%
%
%*************************************************************************
**

function [Azimuth]= Calculate_azimuth
(date_time,latitude,longitude,dif_GMT,summer_advance)

Azimuth = 0; %Initialise sun elevation angle to zero
declination = 0;
dn = 0;
light_savings = 0;

% calculate day number

date_time_vec = datevec(date_time);

year = date_time_vec(1);
month = date_time_vec(2);
day = date_time_vec(3);

date=[year,month,day];
date_num=datenum(date);

hour = date_time_vec(4);
min = date_time_vec(5);
sec = date_time_vec(6);

% Local standard time
time=[hour,min,sec];
time_num=time(1)+time(2)/60+time(3)/3600;

year_ref = year-1;
start_year_str = [year_ref,12,31];
start_year= datenum(start_year_str);

dn=date_num-start_year;

% calculate declination

declination = 23.45 * sind ((360/365) * (dn+284));


% ** Start calculation of hour angle w **

%Equation of Time (in min)

B = (360/365)*(dn-81);

EOT =(9.87*sind(2*B))-(7.53*cosd(B))-1.5*sind(B);

% Local Standard Meridian Time LSMT (in degrees)
```

```
long_standard_m = 15*(dif_GMT);%Difference of local time with GMT -
Greenwich


% Time Correction Factor (in min)

TC = 4*(long_standard_m-longitude)+EOT;

% Consider light savings in summer
if summer_advance == 1
    if 84<dn<301 % 28 oct 2011 end light saving, 25 march 2012 begins
        light_savings=1;
    else
        light_savings=0;
    end
end

% Solar Time (in hours)

ST = time_num + (TC/60)-light_savings;

% Hour angle w (in degrees)

w = 15*(ST-12);

% ** Finish calculation hour angle w **


% calculate sun elevation angle

Sun_elevation_angle =
asind(((sind(declination))*(sind(latitude)))+((cosd(declination))*(cosd(l
atitude))*(cosd(w))));

Azimuth = asind((cosd(declination)*sind(w))/cosd(Sun_elevation_angle));

end
```

```
%********************** SD_Pyrheliometer function************************
%
% SD_Pyrheliometer.m
%
% Function that calculates the sunshine duration as the period composed
by
% the subperiod in which the direct solar irradiance is above 120W/m2.
% The sub-period is 1 min. Input is a vector with direct solar irradiance
% every minute for a day.
%
% Marta Vivar, 12/02/2013
% Variable dictionary
% SD_Pyrhel Calculated number of sunshine hours in hours
% Solar_data Vector with direct solar irradiance every minute of a day
% i index for the 'for' loop
%*************************************************************************
**

function [SD_Pyrhel]= SD_Pyrheliometer_2 (Solar_data)
SD_Pyrhel = 0; %Initialise number of sunshine hours to zero
for i=1:length(Solar_data) %For each minute,
    if ~isnan(Solar_data(i))
        if Solar_data (i)>120 % if direct solar irradiance above 120W/m2
            SD_Pyrhel = SD_Pyrhel + 1; %then increase number of hours by
1min
        end
    end
end
SD_Pyrhel=SD_Pyrhel/60;
end
```

```
%********************** SD_Slob_Monna function ************************
%
% SD_Slob_Monna.m
%
% Function that calculates the sunshine duration using the Slob and Monna
% pyranometric algorithm.
% Input is a vector with global horizontal solar irradiance each minute
% for a day.
%
% Marta Vivar, 12/02/2013
% Variable dictionary
% SD_Slob_Monna Calculated number of sunshine hours in hours
% Solar_data Vector with global solar irradiance every minute of a day
% i index for the 'for' loop
%
%
%
%*************************************************************************
**

function [SD_Slob_Monna]= SD_Slob_Monna_2
(time,Solar_data,latitude,longitude,dif_GMT,summer_advance)

SD_Slob_Monna = 0; %Initialise number of sunshine hours to zero

I_0 = 1367; % for extraterrestrial irradiance, W/m2

i = 0;
j = 0;
sun_elev_angles=0;
% Calculate sun elevation angle for all the data, then mean in 10-min
% intervals.

sun_elev_aux = 0;

for j=1:length(time)

% First calculate the solar zenith angle cosine, or the
% sun elevation angle sin.

sun_elev_aux =
Calculate_sun_elevation_angle(time(j),latitude,longitude,dif_GMT,summer_a
dvance);

if j==1
    if sun_elev_aux<0
        sun_elev_angles=0;
    else
        sun_elev_angles=sun_elev_aux;
    end
else
    if sun_elev_aux<0
        sun_elev_angles = [sun_elev_angles,0];
    else
        sun_elev_angles = [sun_elev_angles,sun_elev_aux];
    end
end

end % for - calculation sun elevation angles
```

```
for i=1:10:length(Solar_data)%For each interval of 10 minutes,

    %Initialise variables to zero
    f = 0;
    T_L = 0;
    SD_10_current_interval = 0;

    sun_elev_10_min_interval = sun_elev_angles(i:i+9);

    sun_elevation_angle = mean(sun_elev_10_min_interval);

    sin_sun_elevation=sind(sun_elevation_angle);


    G_10_min_interval = Solar_data(i:i+9);

    %****************
    G = mean(G_10_min_interval(~isnan(G_10_min_interval(1,:))));

    G_0 = I_0*sin_sun_elevation;

    G_G_0 = G/G_0; % G/G_0

    if ~isnan(G_G_0(1,1))

    if sin_sun_elevation<0.1 % sun elevation less than 5.7º, sin <0.1
        f = 0;
    else
        if sin_sun_elevation<0.3 % sun elevation between 5.7º and 17.5º
            T_L = 6;



            Comp = 0.2 + (sin_sun_elevation/3) + exp(-
T_L/(0.9+(9.4*sin_sun_elevation)));

            if G_G_0 <= Comp
                f = 0;
            else
                f = 1;
            end

        else % sun elevation above 17.5º

            % calculate G_max, 10 min interval


            G_max = max(G_10_min_interval);
            G_min = min(G_10_min_interval);

            G_0 = I_0*sin_sun_elevation;

            G_max_G_0 = G_max/G_0; %G_max/G_0

            if G_max_G_0 < 0.4
                f = 0;
```

```
            else
                G_min_G_0 = G_min/G_0; %G_min/G0
                T_L = 10;
                Comp_2 = 0.3 + exp((-T_L)/(0.9+(9.4*sin_sun_elevation)));

                if G_min_G_0 > Comp_2
                    f=1;
                else
                    if (G_max_G_0 > Comp_2)&&((G_max-G_min)<(0.1*G_0))
                        f = 1;
                    else
                        %calculate c

                        if (1.2*G_min < 0.4)
                            D = 1.2*G_min;
                        else
                            D = 0.4;
                        end

                        T_L = 4;

                        I = I_0*exp((-
T_L)/(0.9+(9.4*sin_sun_elevation)));

                        c = (G-D)/(I*sin_sun_elevation);

                        if c < 0
                            f = 0;
                        elseif c <= 1
                            f = c;
                            else
                            f = 1;
                        end

                    end

                end
            end


        end

    end % calculation f in 10-min intervals
    end
    SD_10_current_interval = f*10;   %current SD for the 10-min interval

    SD_Slob_Monna = SD_Slob_Monna + SD_10_current_interval;

end %for - main

SD_Slob_Monna = SD_Slob_Monna/60; %in hours per day

end
```

```
%********************** SD_Olivieri function ************************
%
% SD_Olivieri.m
%
% Function that calculates the sunshine duration using the Olivieri
% pyranometric algorithm.
% Input is a vector with global horizontal solar irradiance each minute
% for a day.
%
% Marta Vivar, 12/02/2013
% Variable dictionary
% SD_Olivieri Calculated number of sunshine hours in hours
% Solar_data Vector with global solar irradiance every minute of a day
% i index for the 'for' loop
%
%
%
%*************************************************************************
**

function [SD_Olivieri]= SD_Olivieri
(time,Solar_data,latitude,longitude,dif_GMT,summer_advance)

SD_Olivieri = 0; %Initialise number of sunshine hours to zero

%I_0 = 1367; % for extraterrestrial irradiance, W/m2

i = 0;
j = 0;
sun_elev_angles=0;
% Calculate sun elevation angle for all the data, then mean in 10-min
% intervals.

sun_elev_aux = 0;

for j=1:length(time)

% First calculate the solar zenith angle cosine, or the
% sun elevation angle sin.

sun_elev_aux =
Calculate_sun_elevation_angle(time(j),latitude,longitude,dif_GMT,summer_a
dvance);

d_n = Calculate_day_number(time(j));

if j==1
    if sun_elev_aux<0
        sun_elev_angles=0;
    else
        sun_elev_angles=sun_elev_aux;
    end
else
    if sun_elev_aux<0
        sun_elev_angles = [sun_elev_angles,0];
    else
        sun_elev_angles = [sun_elev_angles,sun_elev_aux];
    end
end
```

```
end % for - calculation sun elevation angles

for i=1:length(Solar_data)%For each interval of 10 minutes,

    %Initialise variables to zero
    f = 0;

    sun_elevation_angle = sun_elev_angles(i);

    sin_sun_elevation=sind(sun_elevation_angle);

    G = Solar_data(i);

    if sun_elevation_angle<3 % sun elevation less than 3º
        f = 0;
    else

        G_0 = 1080*(sin_sun_elevation^1.25);

        A=0.73;
        B=0.06;

        F = A + B*cosd(360*d_n/365);

        if G>G_0*F
            f=1;
        else
            f=0;
        end
    end

   SD_Olivieri = SD_Olivieri + f;

 end % calculation f

 SD_Olivieri = SD_Olivieri/60; %in hours per day

end %for - main
```

```
%********************** SD_Hinssen_Knap function ************************
%
% SD_Hinssen_Knap.m
%
% Function that calculates the sunshine duration using the Hinssen and
Knap
% pyranometric algorithm.
% Input is a vector with global horizontal solar irradiance each minute
% for a day.
%
% Marta Vivar, 12/02/2013
% Variable dictionary
% SD_Hinssen_Knap Calculated number of sunshine hours in hours
% Solar_data Vector with global solar irradiance every minute of a day
% i index for the 'for' loop
%
%
%
%*************************************************************************
**

function [SD_Hinssen]= SD_Hinssen_Knap_2
(time,Solar_data,latitude,longitude,dif_GMT,summer_advance)

SD_Hinssen = 0; %Initialise number of sunshine hours to zero

I_0 = 1367; % for extraterrestrial irradiance, W/m2

i = 0;
j = 0;
sun_elev_angles=0;
% Calculate sun elevation angle for all the data, then mean in 10-min
% intervals.

sun_elev_aux = 0;

for j=1:length(time)

% First calculate the solar zenith angle cosine, or the
% sun elevation angle sin.

sun_elev_aux =
Calculate_sun_elevation_angle(time(j),latitude,longitude,dif_GMT,summer_a
dvance);

if j==1
    if sun_elev_aux<0
        sun_elev_angles=0;
    else
        sun_elev_angles=sun_elev_aux;
    end
else
    if sun_elev_aux<0
        sun_elev_angles = [sun_elev_angles,0];
    else
        sun_elev_angles = [sun_elev_angles,sun_elev_aux];
    end
end
```

```
end % for - calculation sun elevation angles

for i=1:10:length(Solar_data)%For each interval of 10 minutes,

    %Initialise variables to zero
    f = 0;
    T_L = 0;
    SD_10_current_interval = 0;

    sun_elev_10_min_interval = sun_elev_angles(i:i+9);


    sun_elevation_angle = mean(sun_elev_10_min_interval);

    sin_sun_elevation=sind(sun_elevation_angle);


    G_10_min_interval = Solar_data(i:i+9);

    G = mean(G_10_min_interval(~isnan(G_10_min_interval(:,1))));

    G_0 = I_0*sin_sun_elevation;

    G_G_0 = G/G_0;

    if ~isnan(G_G_0(1,1))

    if sin_sun_elevation<0.3 % sun elevation less than 17.46°

        if G/G_0 <0.4
            f=0;
        else
            if G/G_0 < 0.5
                f = ((G/G_0)-0.4)/0.1;
            else
                f = 1;
            end

        end

    else

        if G/G_0 < 0.45
            f = 0;
        else
            if G/G_0 < 0.6
                f = ((G/G_0)-0.45)/0.15;
            else
                f = 1;
            end
        end
    end
    end
    SD_10_current_interval = f*10;   %current SD for the 10-min interval

    SD_Hinssen = SD_Hinssen + SD_10_current_interval;

end % calculation for- in 10-min intervals
```

```
    SD_Hinssen = SD_Hinssen/60; %in hours per day
end
```